Spongy Polydimethylsiloxane Preparation and its Applications for Soft Robotics

A THESIS SUBMITTED TO

THE GRADUATE SCHOOL OF ENGINEERING AND

SCIENCE

OF BILKENT UNIVERSITY

IN PARTIAL FULFILLMENT OF THE REQUIREMENTS FOR

THE DEGREE OF

MASTER OF SCIENCE

IN CHEMISTRY

BY

MUHAMMAD ILYAS

September 2022

Spongy Polydimethylsiloxane Preparation and its Applications for Soft Robotics

MUHAMMAD ILYAS

September 2022

We have certified that we have read the thesis and that, in our opinion, it is fully adequate, in scope and quality, as a thesis for the degree of Master of Science.

Bilge BAYTEKİN (Advisor)

Burak ÜLGÜT

Özgül Persil ÇETİNKOL

Approved for the Graduate School of Engineering and Science:

Orhan ARIKAN
Director of the Graduate School

Abstract

Spongy Polydimethylsiloxane Preparation and its Applications for Soft Robotics

Muhammad Ilyas

M.S. in Chemistry

Advisor: Dr. Bilge Baytekin

Soft Robotics has come to the fore in the last decade as a new way of conceptualizing, designing, and fabricating robots. Soft materials empower robots with locomotion, manipulation, and adaptability capabilities beyond those possible with conventional rigid robots. The field of soft robotics utilizes compliant architects to minimize machine complexity and approach biological systems' mechanical and sensing capabilities. Recently, soft (i.e., compliant, and extensible) materials and structures have enabled machines capable of versatile locomotion as well as analogs for caterpillars, fish, jellyfish, and octopus tentacles. With reduced control complexity, these soft machines allow natural motion through continuous deformation and interact gently with fragile objects. The porous, elastic polymers are attracting the attention of researchers in this regard. Here, we demonstrate a facile method for fabricating the lightweight, low-density, elastic PDMS spongy material using sugar as a porogen for different soft robotics applications. The poroelastic material can hold the weight of the robot’s body as legs. This PDMS sponge also successfully demonstrates the application of oil-water separation material for swimming robots. The recyclability of absorption and ability to separate oil from water at different pH levels demonstrate that this material can be effectively used in various conditions. A solvent-light responsive biomimetic soft gripper engineering was investigated by changing the degree of crosslinking and successfully manipulating the swelling of PDMS porous material in different organic media. This soft gripper can lift and release objects in response to NIR light.

ÖZET

Muhammad Ilyas

M.S. in Chemistry

Advisor: Dr. Bilge Baytekin

Esnek robotlar, son on yılda robotları kavramsallaştırmanın, tasarlamanın ve üretmenin yeni bir yolu olarak öne çıkmaktadır. Esnek malzemeler sayesinde bu robotlar, geleneksel sert yapıda bulunan robotlarla mümkün olanın ötesinde hareket, manipülasyon ve uyarlanabilirlik anlamında geliştirilmektedir. Esnek robotik alanı, makine karmaşıklığını en aza indirmek ve biyolojik sistemlerin mekanik ve algılama yeteneklerine yaklaşmak için uyumlu mimarilerden yararlanmaktadır. Son zamanlarda, esnek (yani uyumlu ve genişletilebilir) malzemeler ve yapılar, çok yönlü hareket kabiliyetine sahip makinelerin yanı sıra tırtıllar, balıklar, denizanaları ve ahtapot dokunaçları için analogları mümkün kılmaktadır. Azaltılmış kontrol karmaşıklığı ile bu esnek makineler, sürekli deformasyon yoluyla doğal harekete izin vermekte ve kırılgan nesnelerle nazikçe etkileşime girmektedir. Bu alanda gözenekli, elastik polimerler araştırmacıların ilgisini çekmektedir. Bu çalışmada, farklı esnek robotik uygulamalar için bir gözenekli malzeme olarak şeker kullanılarak, süngerimsi yapıya sahip düşük yoğunluklu, elastik PDMS imal etmek için kolay bir yöntem geliştirilmiştir. Bu gözenekli elastik malzeme, robotun vücudunun ağırlığını bacaklar da olduğu gibi tutabilmektedir. Aynı zamanda PDMS süngeri, yüzen robotlar için yağ-su ayrılması işlemini de başarıyla gerçekleştirmektedir. Absorpsiyonun geri dönüştürülebilirliği ve farklı pH seviyelerinde yağı sudan ayırma yeteneği, bu malzemenin çeşitli koşullarda etkili bir şekilde kullanılabileceğini göstermektedir. Çözücü ışığa duyarlı bir biyomimetik esnek tutucu mühendisliği, çapraz bağlanma derecesi değiştirilerek ve PDMS gözenekli malzemenin farklı organik ortamlarda şişmesini başarıyla manipüle ederek araştırılmıştır. Bu esnek tutucu, NIR ışığına tepki olarak nesneleri kaldırabilmekte ve serbest bırakabilmektedir.

Acknowledgments

First of all, I pay my gratitude to Almighty Allah, the Lord, and Creator of the heavens and earth. He is certainly the supreme patronage of my life. This opportunity of pursuing my masters at Bilkent University is one of His countless blessings upon me.

I would then like to thank my advisor, Dr. Bilge Baytekin for her guidance and encouragement over the years, and for always reminding me to consider a problem at its most basic, fundamental level. I am particularly grateful for her understanding and support of my involvement in activities outside of the lab, which allowed me to develop the nontechnical skills needed to advance my career. I am extremely thankful for giving me the opportunity to excel in my field and for believing in me.

I would also like to thank Dr. Esma for all of her support, insight guidance, and assistance in my experiments and for showing me new ways to bring the best results. Also, I am grateful to Dr. Joanna Kwiczak for helping me out whenever I got stuck somewhere in my work. A huge thank you goes to my friend Hamid Ali who also helped me a lot in ATR and XPS analysis and keep me motivated always, and Muhammad Ahsan for helping me out in the difficult part of this journey. Furthermore, I would like to thank all the former and current group members for making the lab environment extremely compatible with conducting research.

I would like to extend my gratitude to the other faculty members of the Department of Chemistry especially Dr. Omar Dag, Dr. Ferdi Kardas, and Dr. Yunus Emre for their time and efforts during the completion of course work for this degree.

Last but not the least, I am highly grateful to all my family members who put lots of effort into bringing me to this stage of my life especially my father and my brother, without their support this journey was impossible. And finally, I would like to acknowledge the support, motivation, and lot of prayers of my fiancé, who was always there to appreciate and encourage me every time.

Table of Contents

List of Figures

List of Tables

Chapter 1

1. Introduction

1.1. Robotics History

The word *Robot* was first used by a Czech playwright, novelist, and journalist named Karl Capek in his 1920s hit play *Rossum's Universal Robot*[1]. Now this word has become so mundane in science and technology these days. Isaac Asimov is credited for the popularization of robotics in his short stories published between 1938 to 1942. He suggested three rules to regulate the behavior of robots[2]:

- A robot may not injure a human being or through inaction allow a human to come to harm.
- A robot must obey orders given to it by humans except when doing so conflicts with the first law.
- A robot must protect its own existence if this does not conflict with the first or second law.

The use of Unimate to assist in the automobile industry by General Motors in 1961 marked the transition of robots from fiction to reality, and since then, their usage in daily life has exploded. Now we find a variety of robotics applications including deep sea and space exploration, search and rescue purposes, military and defense industry, medical and education industry, etc. In all cases, the purpose of robots' actions is to duplicate or enhance human actions or to perform tasks more efficiently in an environment where it is all impossible for humans[3].

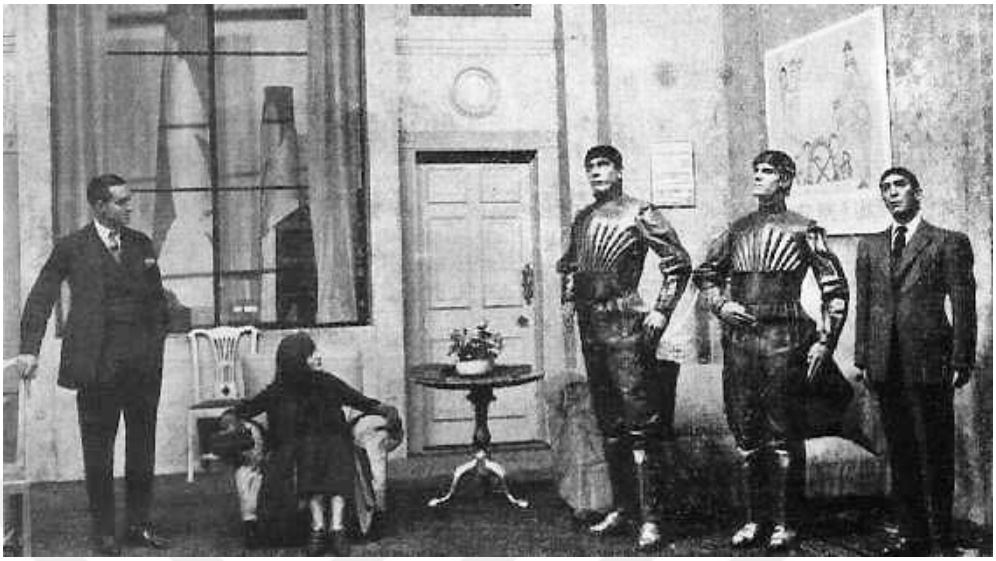

Figure 1: A scene from ***Rossum's Universal Robots***, showing three robots[4]

The advancement of technology led the application of robots in all aspects of life. So, the design and structure of robotics body is determined by the application and degree of exertion it goes through during performing various tasks. The robots can be divided into four different categories depending upon their applications[5]: 1) highly specialized robots with advanced technologies for specific tasks such as space and deep-sea exploration, often comes with intelligence to deal with unstructured environment 2) highly accurate, reliable, and efficient robots for industrial applications; 3) toy robots for children to accompany in a friendly environment; 4) low cost and attractive robots for education and commercial uses.

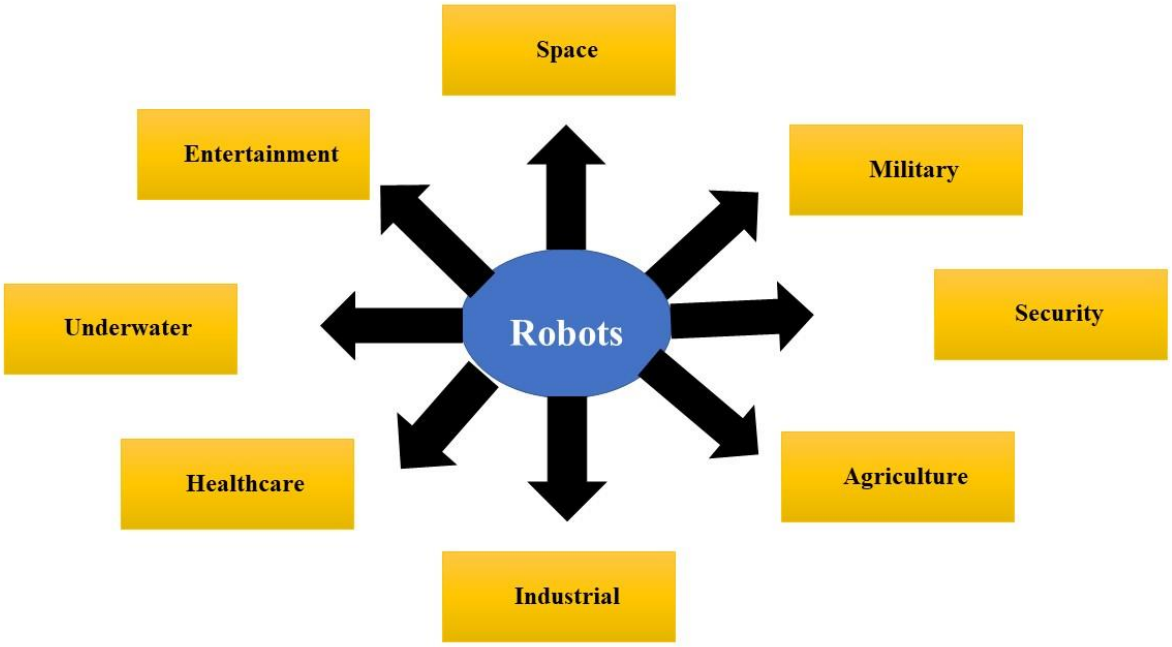

Figure 2: Applications of robots in everyday life[6]

Each category of robots involves innovative technology for performing different jobs with high precision and efficiency to help humankind in variety of areas. The low-cost and attractive robots are marking themselves as the most prospective robots to meet the popular demand. Billions of dollars are being flushed for the research over design, development, engineering, and applications of aesthetic robots for better operation and comprehensive systematics[5]. The other part of exploration is to make these gadgets cost-effective and recyclable, as the environmental degradation is increasing with the advancement of technology over the last few decades[7]. Researcher are looking for sustainable and biodegradable alternatives for these machines to tackle the issue of global warming and cost-reduction. But the application and operative systems of robots determine the degree of sustainability and recyclability it can achieve during manufacturing process.

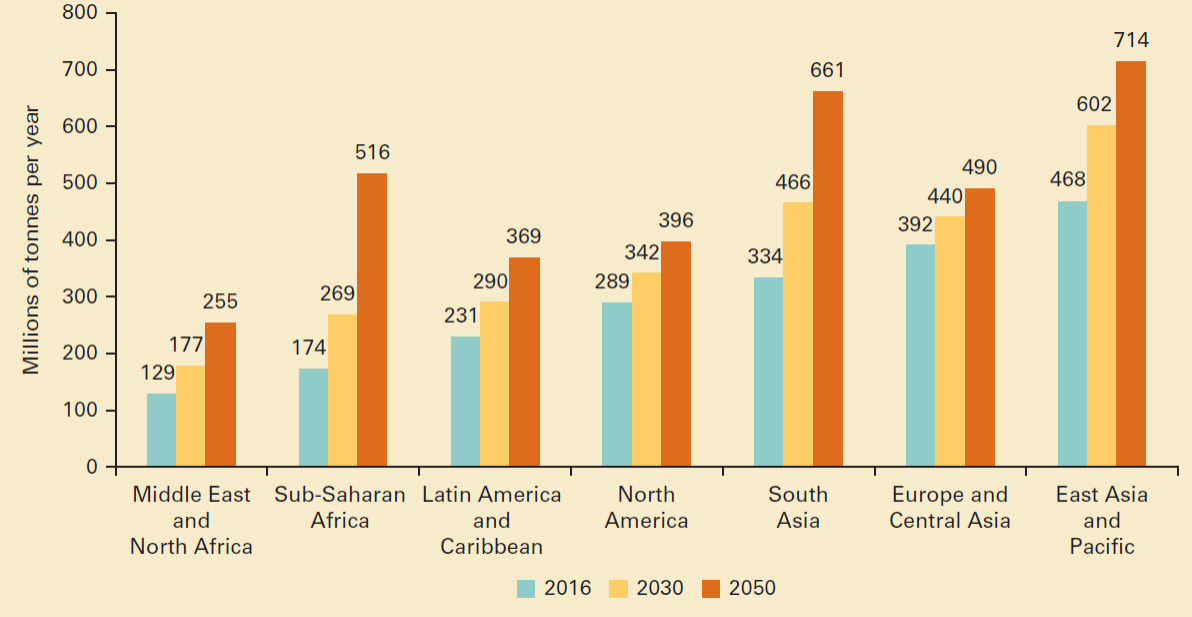

Figure 3: The projected waste generation by different regions in the world. Source: https://datatopics.worldbank.org/what-a-waste

1.2. Soft Robots

Soft robotics evolved as a new sub field in robotics world in last decade. The exploitation of deformability of soft structures by animals for performing different tasks efficiently inspired the robot's engineers. The mechanical design of animals requires soft materials and it coevolved with the nervous system to come up with an integrated neuromechanical system. These soft materials not only provide advantages for dealing with unstructured environment but also endow other marvelous characteristics such as deformability, high compliance, flexibility, distribution and lowering of the impact of stress etc.[8]. The ecological niches are determinant for the evolutionary course of developing stiffness or hardness. The animals that do not require the high speed and impact of stress for performing specialized task tend to develop soft bodies. For example, octopus can squeeze its body and caterpillars can stick to their host plants for survival. Jelly fishes pump their bodies through water.

Figure 4: (Left) An Octopus moving in an ocean. (Right) A jellyfish propelling itself in a sea. The soft tissues and architecture of these creatures are perfect models for soft robotic systems.

Despite of all the stunning characteristics, soft biological materials have few disadvantages. The smaller size, support of external media for support, and ecological confinement to a specific niche render soft structured animals few limitations in an alien environment. For example, all large soft invertebrates are found in water (jellyfish, octopus), and underground earthworms. So, material design, selection, and integration in robots' body for softness often come with great challenges. Conventional approaches have been failed to tackle the problems with soft material engineering and this is all due to intrinsic soft mechanical properties of such materials. To produce versatile functionalities of such soft robots, two objectives should be achieved: (I) replacing modular systems (separate hardware for motor, controller, sensors, etc.) with fully integrated materials architectures that merges these functionalities; and (ii) replacing hard and piecewise rigid mechanisms with soft-matter (e.g. elastomer, gels, fluids, biomatter) that is in physical contact with other objects[9].

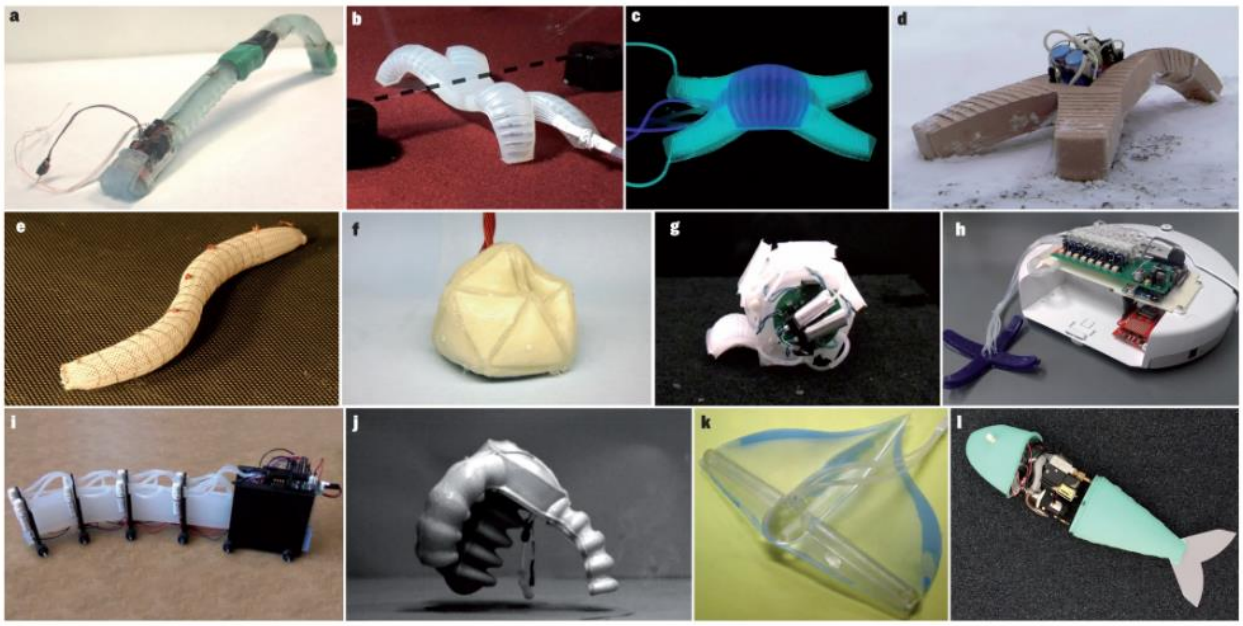

Figure5: Mobile, soft robot systems inspired by a variety of living systems.[10] **, a**) Caterpillar-inspired locomotion. **b**) A multi-gait quadruped **c)**, Active camouflage **d**) Walking in hazardous environments **e)** Worm-inspired locomotion **f**) Particle-jamming-based actuation **g**) Rolling powered by a pneumatic battery **h**) A hybrid hard–soft robot **i**) Snake-inspired locomotion **j**) Jumping powered by internal combustion **K**) Manta-ray inspired locomotion **I)** An autonomous fish

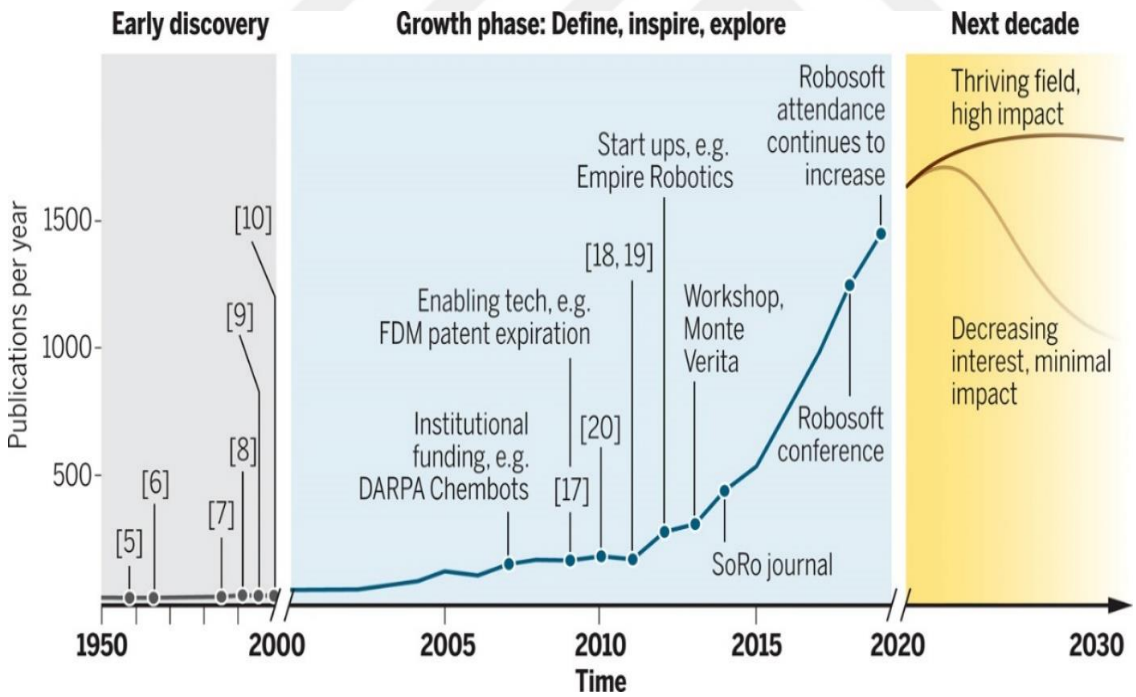

Figure 6: Evolution of soft robotics literature over the last few years[9]

1.3. Materials for soft robots

Soft materials, the key enablers for creating soft robot bodies, must possess specific salient characteristics for applications. Young's modulus which defines axial loading and small deformations to evaluate mechanical properties for various materials, is nonetheless a useful measure of the stiffness of materials used in the fabrication of soft robotic systems[11]. Materials commonly used in robotics (metals or hard plastics) have moduli in the order of 10^9–10^{12} pascals, whereas natural organisms are often composed of materials (skin or muscle tissue) with moduli in the order of 10^4–10^9 Pa (orders of magnitude lower than their engineered counterparts)[12]. To demonstrate the features and functionalities of soft robots, body of machines must be primarily composed of materials with moduli in the range of that of soft biological materials. The flexibility, stretchability, and conformability of materials similar to living organisms are advantageous for a considerable reduction in the harm that could be inadvertently caused by robotic and promotes their potential for safer interaction with humans. The soft architecture of such machine gives ability to adapt different shapes and perform various tasks with improved mobility and efficiency over different terrains.

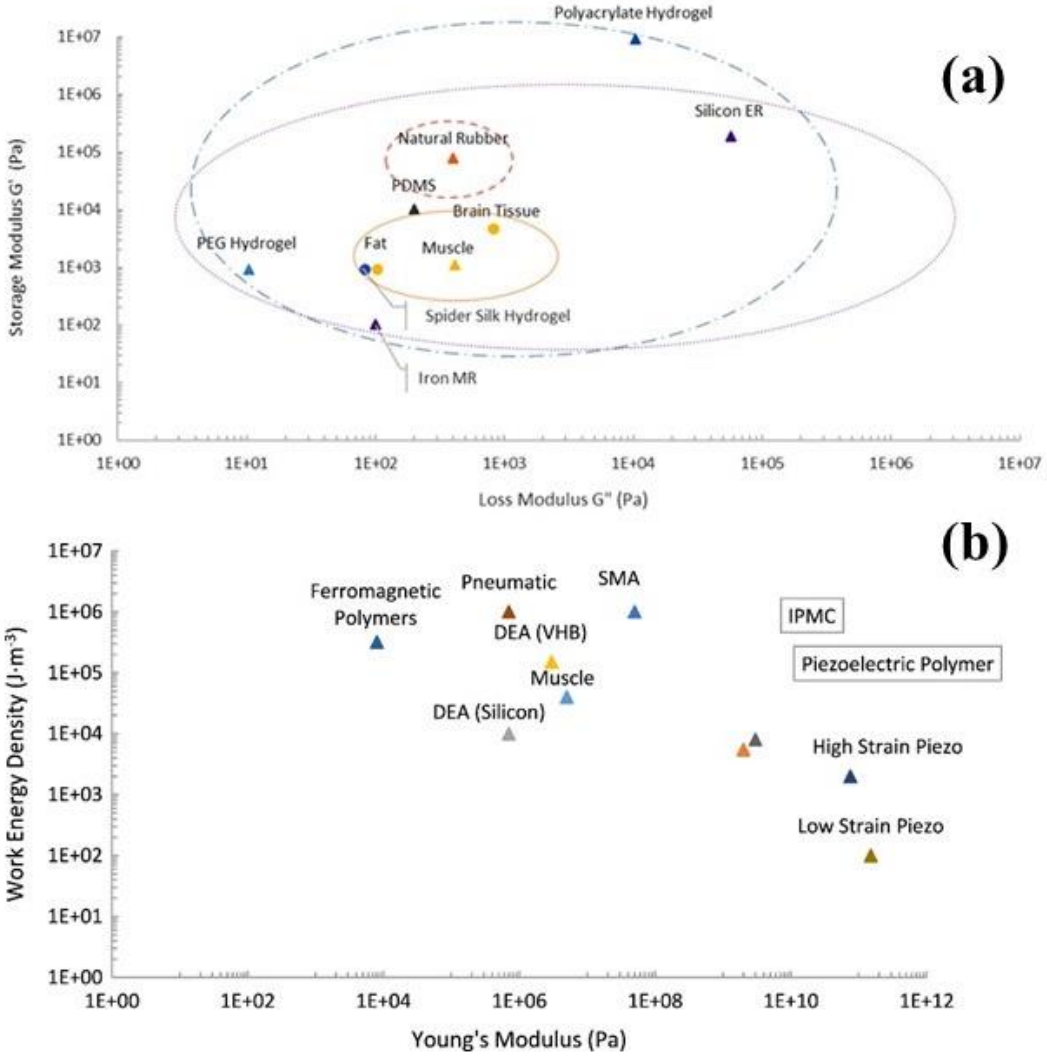

Figure 7: a) Approximation of storage modulus vs young's modulus of varied materials b) work energy vs young's modulus of synthetic materials for industrial applications[9]

Advanced functional materials are being extensively investigated for soft robotics, and a variety of soft robotic systems that encompass locomotion robots, grippers and sensors have been designed and fabricated[13][14][15]. These materials can be triggered by external stimuli such as heat,

light, electric fields, and magnetic fields to produce large deformations like isotropic/anisotropic swelling and variable stiffness[16][17]. For example, Dielectric elastomers (DEs) , widely used as electroactive polymers (EAPs), which can produce large strain through the Maxwell stress induced by electric activation[18]. Shape memory polymers (SMPs)[19] and liquid crystal elastomers (LCEs)[20] offer reversible, programmable deformations and actuation outputs triggered by external stimuli (mostly heat or light) through vitrification/crystallization of switching domains and reconfiguration of liquid crystal mesogens, respectively. The plasticity, excellent biocompatibility, transparency and conductivity of hydrogels with high water content are prominent features to be exploited for soft robotic applications[21]. Similarly, to provide remote manipulation and locomotion guidance for soft robots in confined workstation, the magnetic materials present an excellent solution in predesigned magnetic fields[22]. However, selection and modifications of these state-of-the-art soft functional materials toward specific soft robotic applications often encounter great challenges[23]. For instance, continuous supply of high voltage and other electrical safety issues raise the concerns for applications of DEs on large scale[18]. SMPs suffer from long transition times owing to the cooling process[13], and the miniaturization and prolonged deformation of LCEs are hard to tackle[24]. Hydrogels are prone to dehydration in dry environments[25] and lose their shape and functionality after certain period of time, whereas the biocompatibility issues of magnetic materials are unfavorable due to intrinsic corrosion[22].

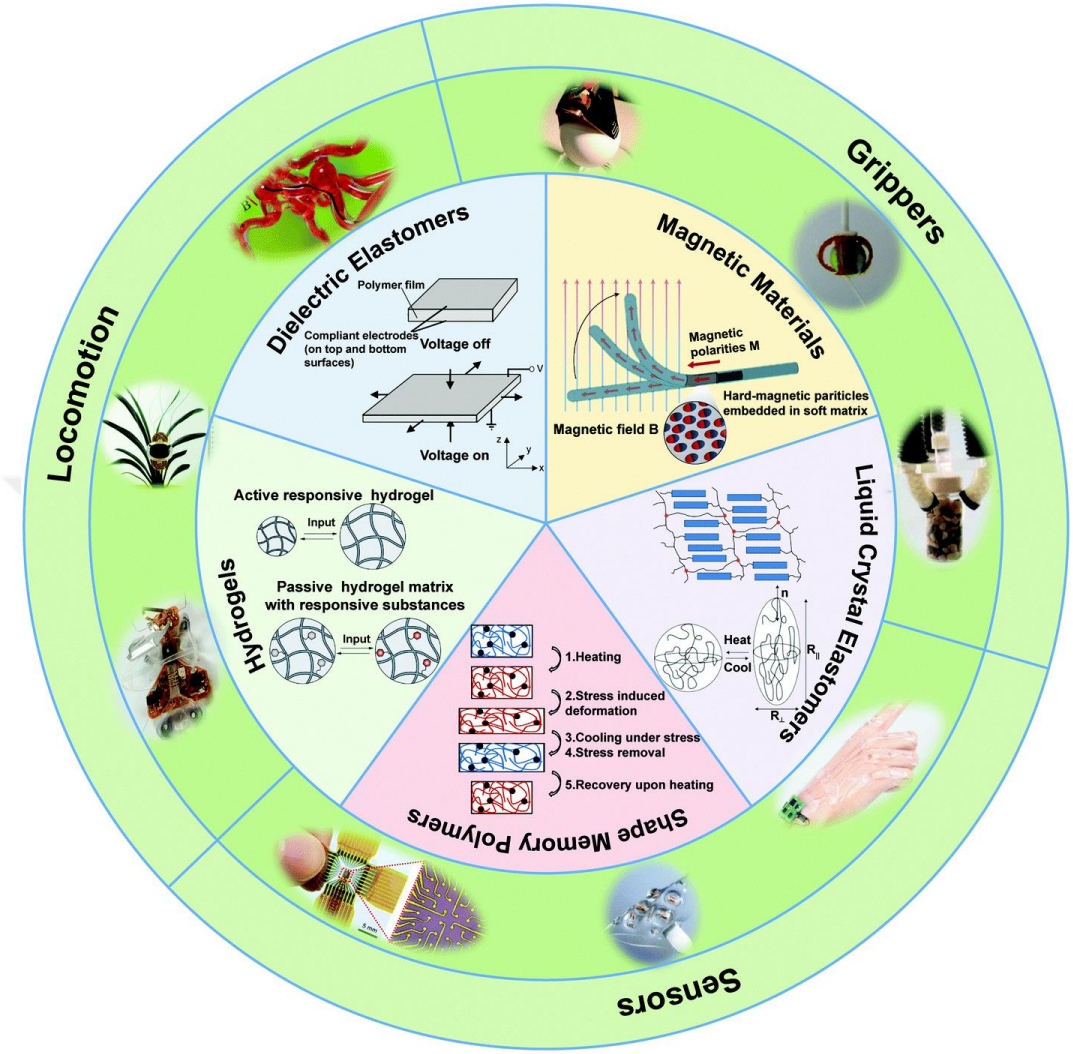

Figure 8: Overview of typical advanced functional materials and their applications for soft robotics[23]

1.4. Polydimethylsiloxane for soft robots

Synthetic polymers especially silicones are efficient material candidate for wide variety of applications like micro-nanofabrication, biomedical industry, aerospace industry, and robotics, etc. In general, polymers with a (-R_2Si-O-) unit are termed silicones, while the (-Si-O-) repeat unit is also called siloxane. The thermal and chemical stability needed for applications in different fields, comes from the strength of the Si-O bond[26][27][28][29]. Several silicone elastomers are

available, Polydimethylsiloxane (PDMS) with brand name *Sylgard 184*® from DOWSIL being the most cited in the scientific literature for various applications in different industries within the last few decades [30][26]. The composition of *Sylgard 184*® is not disclosed by the manufacturer. However it is reported to be as follows: Base: dimethylsiloxane oligomers with vinyl end groups (>60%), silica filler (dimethylvinylated and trimethylated silica, 30–60%), tetra(trimethylsiloxy) silane (1–5%) and ethylbenzene (<1%), and a platinum catalyst. Curing agent: a cross-linking agent (dimethyl methylhydrogen siloxane, 40–70%) and an inhibitor (tetramethyl tetravinyl cyclotetrasiloxane 1–5%)[31].

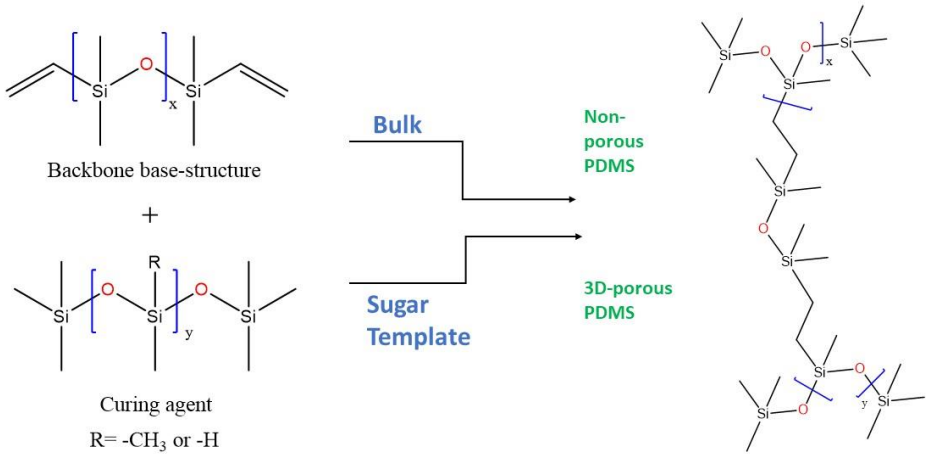

Figure 9: Structure of PDMS. The backbone of chains contain (-O-Si-O-) functionality, which gives it flexibility and is important for many physio-chemical properties[29].

In PDMS, the siloxane backbone is flexible, and it allows the methyl groups to be present at the surfaces and interfaces. This arrangement and rearrangement process of chains permits the flexibility and intactness of structure under high pressure[32]. Excellent physical properties i.e., optical transparency, biocompatibility, hydrophobicity, low surface energy, and electrical

insulation make PDMS an outstanding material candidate for numerous novel applications in myriad of fields[33][34][29]. PDMS with the standardized ratio of 10:1 with its curing agent, has a modulus of elasticity of G = 250 kPa, due to its low glass transition temperature (T = −125 ℃); low change of modulus of elasticity with temperature variation (1.1 kPa/C); small temperature variations of the physical constants (except for thermal expansivity $\alpha = 20 \times 10^{-5}$ k−1k−1); high dielectric strength (14 V/μm); a wide temperature range (−100 ℃ to 100 ℃) and low chemical reactivity[33]. Due to all these outstanding physiochemical and mechanical properties, PDMS is a promising candidate for soft robotics applications.

Characteristics	***Value***	***Reference***
Optical transparency	240-1100 nm	[35]
Surface tension	21-22 mN/m	[27]
Glass transition temperature	-125 C^0	[27]
Electrical conductivity	2.9 E+14 Ω*cm	[36]
Heat conductivity	0.27 W/m*K	[36]
Young's elastic modulus E	~1-3 MPa	[37]
Surface tension	21 mN/m	[27]
Water vapor diffusion coefficient	~1000–6000 $\mu m^2\ s^{-1}$	[38]
Oxygen diffusion coefficient	~2000–4000 $\mu m^2\ s^{-1}$	[39]
CO_2 diffusion coefficient	~1000 $\mu m^2\ s^{-1}$	[40]

Table 1: Physical properties of PDMS. All these characteristics make PDMS an excellent substituent for various industrial applications.

To achieve maximum efficiency, low power consumption, and specific functionalization of various parts of soft robots, these materials are of light weight, low density, and possess a certain degree of functionalities without compromising over the mechanical properties**.** Keeping these characteristics in view, porous/spongy polymers can be substitutes for such building materials in robotics architectures. Porous/spongy materials are not only light in weight and low in density, but also can be functionalized for specific task performance due to their larger surface to area ratios. Especially, PDMS sponges are finding quite applications in various fields these days due to their flexibility, biocompatibility, ease of production, and excellent mechanical properties. The pore size, degree of porosity, and interconnection of pores distribution solely depends upon different methodologies for pore formation[41]. PDMS sponges offer promising applications in electronics, sensors, energy storage and conversion, oil/water separation, biomedical engineering and many other fields are being explored for potential use[42][41][43][44][45].

In literature, many studies have been reported where PDMS sponge have been applied as various parts of soft robots. For example, Shao et al. developed 3D porous carbon nanotubes PDMS sponge based stimuli-responsive actuator, which realizes both electrothermal and electrochemical actuation[46]. Wang et al. reported elastomeric sponge based sensor that can respond to and distinguish pressure, strain, and temperature stimuli[47]. These kinds of porous and elastic sensors find application in soft wearable electronics and electronic components of soft robots. Peng et al. proposed a strategy to design and fabricate porous conductive PDMS composites of silver-carbon nanotube and reduced graphene oxide by simple dip-drying method[48]. Murray et al. designed

open-celled, elastomeric PDMS foam, which is 3D pneumatic soft machine actuator, and can find its application as fluid pumped, artificial human heart. This poroelastic architecture can pulsate, and maintain the constant flow pressure ($v = 430$ mL min^{-1})[49].

1.5. Application of PDMS Sponges for water Treatment

The availability of clean water is vital for living creatures [50]. The safety of mankind and other ecological systems have been threatened by the disposal of tons of oily wastewater, which is due to growing industrialization over the past few decades[51][52]. The strong cohesive forces between oil and water make oil spill remediation an expensive and complicated process[53]. Keeping these challenges in view, the researchers are working to come up with a solution that is cheap, easy, and can be applied on large scales. Currently, the following four main approaches are being employed to tackle the problem:

- *In-situ* burning[54] where oil is burnt on the surface of standing water.
- Dispersants[55] where oil is chemically broken into very small droplets spreading oils throughout the water column and allowing for more facile digestion by microbes.
- Booms and skimmers[56] where oil is contained by the booms and then skimmed via pumps.
- Sorbents[57] where is oil absorbed through porous materials.

In order to meet the definition of sustainability, all the above-mentioned methods have some drawbacks and need more improvements for better efficiency. *In-situ* burning leads to carbon emissions and dispersants pose risks to marine life[54][55]. The roughness of water and thickness of the oil layer limits the use of skimmers[58]. Though sorbents are considered a green solution,

the cost of sorbents is comparatively high (oil spill cost is ~ $5/ gallon of oil). As well as the treatment of solid waste generated is another challenge of using this method.

Thus, the oil recovery from the current oil remediation techniques seems to be a tiresome job at best and needs appreciable amounts of resources to meet the sustainability and requirement of deployment. Cost-effectiveness, selectivity for oil, and efficiency of removing oil from spill areas render all present approaches inefficacious. To overcome all such drawbacks, other solutions should be sought out, which could satisfy all the requirements of materials and methods that are not expensive and can be scalable, and benign to the marine ecosystem.

Due to their highly porous structure, high absorption capacities, and larger separation efficiencies, the three-dimensional (3D) porous materials[59][60] have been an excellent candidate for this purpose. Sponges[61][62][63][64], foams[65][66], aerogels[67][68][69][70] etc. are polymer-based materials with 3D porous structures widely used for oil/water separation. Diversity in porosity, tunable surface wettability, and excellent mechanical strength of these materials differentiate from others for oil spill remediation[71][72][73][74]. The separation of absorbed oil from these materials depends upon the mechanical compressibility, and retention of porosity as well as mechanical durability on repeated absorption- squeezing is important for recyclability[75].

Incorporation of inorganic nanostructures to these 3D porous materials not only increases the mechanical properties but also gives functionalization and much higher absorption capacities. In order to develop mechanical robust sponges for oil/water separation, recently many strong materials like graphene, graphene oxide, wood, and carbon nanotubes etc. have been employed by bottom up and chemical treatment schemes. Owing to its layered structure and great mechanical

strength, graphene has been extensively used to improve the mechanical characteristics of composite materials[76][77][78].

Nevertheless, incorporation of nanomaterials increased the mechanical strength, it also gave rise to other defects like increased brittleness, fragility, and loss of porous structure in composite materials and higher amount of stress was required for a certain amount of strain to desorb the oil and other organic liquids. As discussed earlier, the outstanding compressibility and retention of porous structure is vital for extrusion of absorbed materials for these spongy structures.

Due to outstanding properties and elastic porous structures, Polydimethylsiloxane (PDMS) sponges have been given considerable attention during past few years for many applications. In general, PDMS is a viscoelastic, biocompatible, and chemically and mechanically robust material with a low glass transition temperature, high cost-effectiveness and good moldability, which ensure that it is acceptable for practical uses[79][80]. High flexibility, non-toxicity, non-flammability, heat and current resistant, low bulk density, and many other excellent properties come from Si-O-Si backbone in PDMS structure[26]. Optical properties, good contour accuracy, non-reactive nature towards many reagents, hydrophobicity and many other properties make it promising candidate for many applications like optical fabrication, micro-nanotechnologies, electrical applications[81][26][82].

The correlation between porosity and pristine features must be achieved for a target specific motive, and for these specific modifications and optimizations of methods are required. Different pore forming strategies have been applied to PDMS for obtaining spongy structure, and these involve template casting, gas leaching, 3D printing, phase separation etc. Each method gives a specific profile of porous structure, and the requisite characteristics are assayed based on pore structure, pore geometry, pore volume, and open/close pore network. The application of these

sponges in different areas depends on the structure of pores, and sometimes for enhanced functionalities, these porous entities are subjected to post modification treatment[43][83][84][71][73].

1.5. The Aim of the Thesis

As summarized in in the above discussion, the materials for soft robots should have light weight, low density, with certain mechanical characteristics, and can be functionalized for specific applications by manipulating chemical architecture. Here, I have synthesized spongy, elastic PDMS using sugar as porogen by previously reported method[85] and found its application to support the body of robot, and a material to separate oil from water for swimming robots. Finally, I have also shown that this PDMS spongy material can be used to design a biomimetic, soft gripper due to anisotropic swelling of bilayer PDMS in hexane and dichloromethane.

The objectives of my research comprise:

- Synthesis of porous, light weigh, low density PDMS material for soft robots.
- The mechanical properties of spongy PDMS should be in the range to support robots' body and various parts for specific applications.
- Application of poroelastic PDMS as an Oil/water separation material for swimming robot, and biomimetic, stimuli-responsive soft gripper

The pore size, porosity, and density of spongy PDMS was found to be dependent on the sugar particle size and concentration in PDMS. The pore size was measured by Scanning Electron Microscopy (SEM). To see the interaction and change in surface binding energy before and after

removal of sugar, Attenuated Total Reflection Spectroscopy (ATR), and X-Ray Photoelectron Spectroscopy (XPS) was done. The mechanical properties were evaluated by Dynamic Mechanical Analyzer (DMA). Water Contact Angle (WCA) was measured to obtain the idea about surface wettability for different solvents, and thermal stability of spongy PDMS was assessed by Thermogravimetric Analysis (TGA).

Chapter 2

2. Materials and Methods

2.1. Materials

Polydimethylsiloxane (PDMS) Sylgard 184 (Sigma-Aldrich), sugar cubes with dimensions 12x16x18 mm and pore diameter 487.76± 118.72 um, small granules sugar (particle diameter 490.92±61.5 um and big granules sugar sponge (particle diameter 852.1± 125.01um). Ethanol, Methanol, Acetone, Paraffin oil, Dichloromethane, Tetrahydrofuran, n-Hexane, Ecoflex Silicone, Plastic cups, Hydrochloric Acid, Sodium Hydroxide, Dimethyl Sulfoxide, Citric Acid, Sodium Chloride, Chloroform, Toluene.

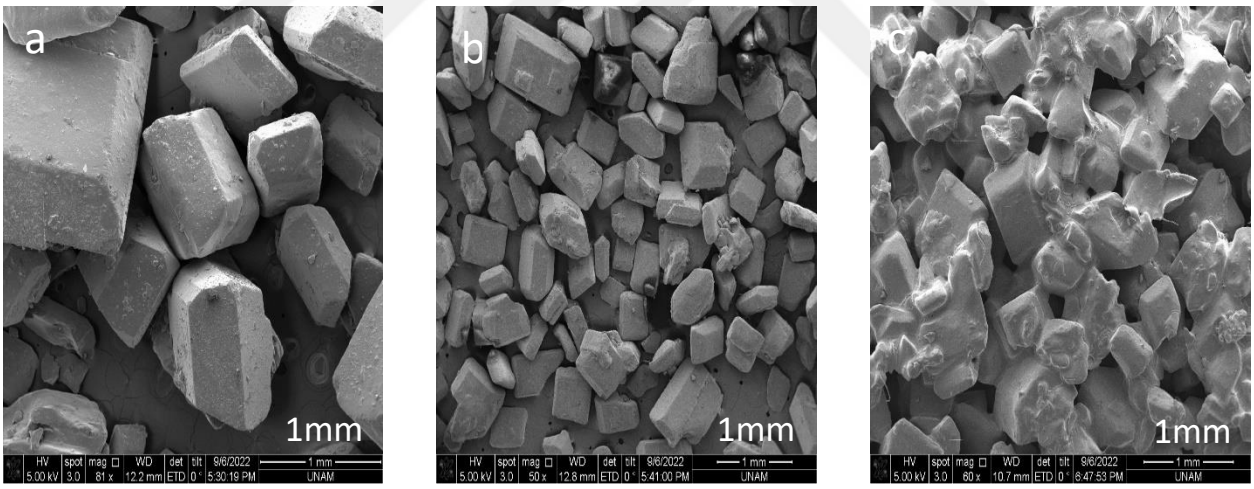

Figure 10: (a) big granules sugar, (b) small granules sugar, (c) cube sugar

2.2. Experimental Method

The formation of polymer foams (sponges) requires distinct methodologies, and the porosity, pore size, and distribution of 3D architectures are determined primarily by the strategies for pore formation. Currently, different methods are used to obtain spongy or foam polymers such as chemical, physical, and mechanical methods. The agent used in all these techniques for pore formation is termed "porogen." In the chemical method, the reactive functional groups are introduced in the monomers of polymers and during the polymerization process, the reaction produces the bi-products as gasses, these gasses function as pore-forming agents (porogen). For example, porous polyurethane is produced in this way. In the physical method, a certain size of crystals is added as porogen to the polymers and when polymers are cured, the dissolution of crystals leaves the void and empty spaces in the architecture. This 3D connected structure depends upon the size of crystals, the number of crystals, and the temperature at which the polymer is cured. If the curing temperature of the polymer is higher than the melting point of crystals added, the non-uniformity in porous is obvious and porosity is affected due to the molten crystals. In the mechanical process, the addition of some volatile solvent, and high spinning are required at a certain temperature. The evaporation of solvent leaves cells and voids in the polymeric structure. In this process, the nature of solvents, their vapor pressure, and compatibility with the polymers are of significant importance for obtaining a uniform and excellent porous structure.

Here we adopted the physical strategy for pore formation in PDMS. The sugar was chosen as a porogen to obtain spongy PDMS material. Sugar which is a cheap material available is soluble in water. It is also an environment-friendly material. The market sugar comes in different forms such as cube shapes, small granules, big granules, star-shaped crystals, etc. Its low melting point (around 180 ^{O}C) and high solubility in water makes its separation from PDMS after pore formation easier.

2.2.1. Preparation of PDMS Sponges by Sugar Particles

Porous PDMS was synthesized by a hard template method, which has already been reported, using sugar particles as porogen[85]. Three distinct types of sugar i.e., 'small granules' sugar, 'big granules' sugar, and cube sugar were used to synthesize the spongy PDMS with varying pore size. In a typical method, the PDMS and curing agent were mixed in 10:1 (W/W) proportion, and then sugar particles were added to the PDMS polymer in 1: 4 (PDMS: sugar) ratio and mixed thoroughly. For this procedure, 12 grams of sugar was added to the 3 grams of PDMS mixture. After this, the mixture was poured into different shaped templates and cured in the oven at 80 ^{O}C for 4 hours. The cured PDMS and sugar mixture was then removed from the template and boiled in distilled water while ultrasonicating for 2 hours. To completely remove the sugar particles, the obtained PDMS sponge was washed with distilled water many times and dried in the oven at 60 ^{O}C for a few hours.

2.2.2. Preparation of PDMS Sponges by Sugar Cubes

For the cube sugar sponge, the PDMS was prepared in 10:1 proportion with the curing agent, and the sugar cubes with average dimensions 15x16x12 mm (lxwxh) were added to the PDMS. Then, the PDMS and cube sugar was put in the vacuum chamber for 30 minutes. The PDMS was sucked up by sugar cubes, and complete soaked cubes were obtained by capillary action movement of PDMS. The sugar cubes soaked with PDMS were put in the oven at 80 ^{O}C for 4 hours, and then washed in distilled water while sonicating at 60 ^{O}C.

The amount of curing agent and curing time determine the mechanical properties of PDMS. So, in all synthesis, the curing conditions were the same i.e., 80 ^{O}C for 4 hours, PDMS: crosslinking agent: sugar granules (10:1:4) by weight.

2.2.3. Design for Soft Gripper

In our design of a soft, biomimetic gripper, we have fabricated a bilayer PDMS architecture, in which a layer is spongy PDMS, which has the ability to swell to a greater extent as compared to the other layer, which can be a bulk PDMS, silicones, or a paper layer. The layer which has low swelling ratios in organic solvents as compared to PDMS sponge, can serve as a strain limiting layer and have the ability to bend the bilayer in a specific direction. This directional bending of bilayer structure can be effectively employed to design a biomimetic soft gripper to lift the objects. Four small granules sugar PDMS sponges with dimensions 16x4x3 mm (lxwxh) were joined on one end, and a A4 size paper with thickness 0.5mm was stick on the sides of 4 sponges in such a way that it gives a plus (+) sign shape. These lengths give the shapes of tentacles. The solvent system for this design was selected after evaluating the swelling ratios of bulk PDMS, spongy PDMS, Ecoflex silicone, and paper in different solvents such as dichloromethane, tetrahydrofuran, and n-Hexane. n-Hexane was finally selected for further testing as it is cheaper and less toxic as compared to the above-mentioned solvents.

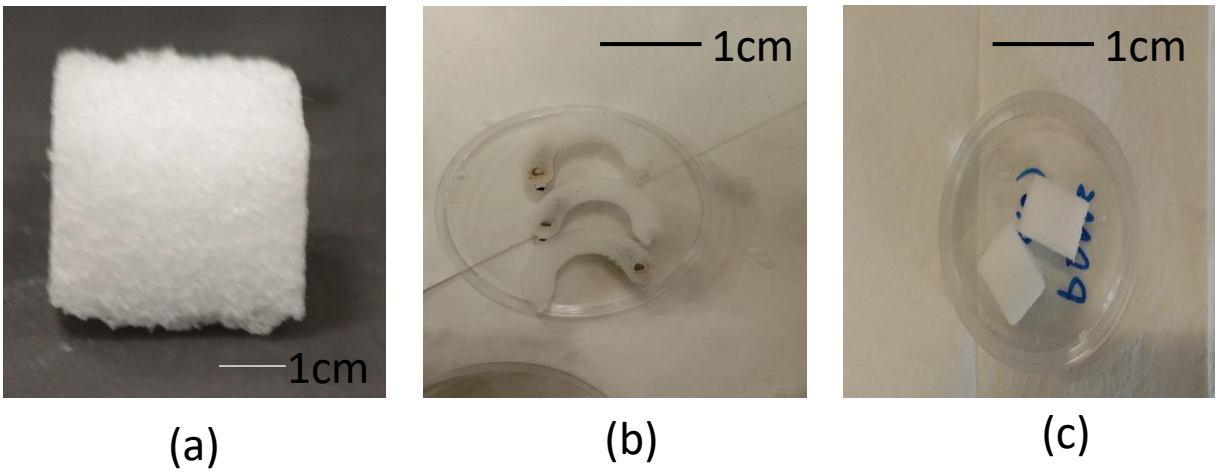

Figure 11: Different shapes of PDMS sponges (a) sugar cube sponge(b) small granules sponge for legs (c) big granules sugar sponge

2.2.4. Percentage Mass Absorption Capacity Measurements

For percentage mass absorption capacity measurements of different solvents, 0.5 g of each sample i.e., bulk PDMS, small granules sugar PDMS sponge, big granules sugar PDMS sponge, and cube sugar PDMS sponge was placed in a beaker with 20 mL of each solvent. The beaker was placed at room temperature i.e., 25 ^{O}C for 30 minutes. The weight difference of dry and wet PDMS samples was measured, and results were recorded by using following formula:

$$\% \text{ Mass Absorption Capacity}$$

$$C = \left(m_2 - \frac{m_1}{m_2}\right) 100$$

$$C = \% \text{ Mass Absorption Capacity}$$

$$m_1 = \text{initial mass}$$

$$m_2 = \text{final mass}$$

2.2.5. Sample Preparation for Oil Recovery at different pH Levels

The absorption efficiencies of different PDMS sponges were also measured at different pH levels. 1N HCl and 1N NaOH solutions were prepared to adjust the pH of distilled water. By adding appropriate amounts of acid and base, 20 mL of water with pH 2, 7, and 12 was obtained. Then 6 g of Paraffin oil was dropped in each water beaker with different pH level. Approximately, 0.3 g of each PDMS sponge sample was placed on the surface of water and moved with tweezer. The weight difference of oil dropped in water and absorbed by sponge was measured and results were recorded by using following formula:

% Oil Recovery

$$C(O) = \left(m_2 - \frac{m_1}{m_2}\right) 100$$

C(O) = *% Oil Recovery*

m_1= mass of Paraffin oil dropped in water

m_2= mass of Paraffin oil absorbed by sponge

The error for water absorption along with oil was calculated and subtracted from the final results.

For this, each PDMS sponge was first dipped in water and mass of water absorbed was calculated, and then this sample was dried in oven to fully evaporate the absorbed water. The dried sample was then used to measure the % oil recovery at different pH levels.

2.2.6. Recyclability of Oil Absorption

The recyclability of absorption capacity of different PDMS sponges was assayed by repeated absorption and desorption of acetone. For this experiment, 5 samples of each PDMS sponge were used. The weight difference of dry and acetone absorbed sponges was measured, and this experiment was repeated for 10 cycles. After completely squeezing the acetone, the sample was washed with ethanol and dried in the oven for next cycle.

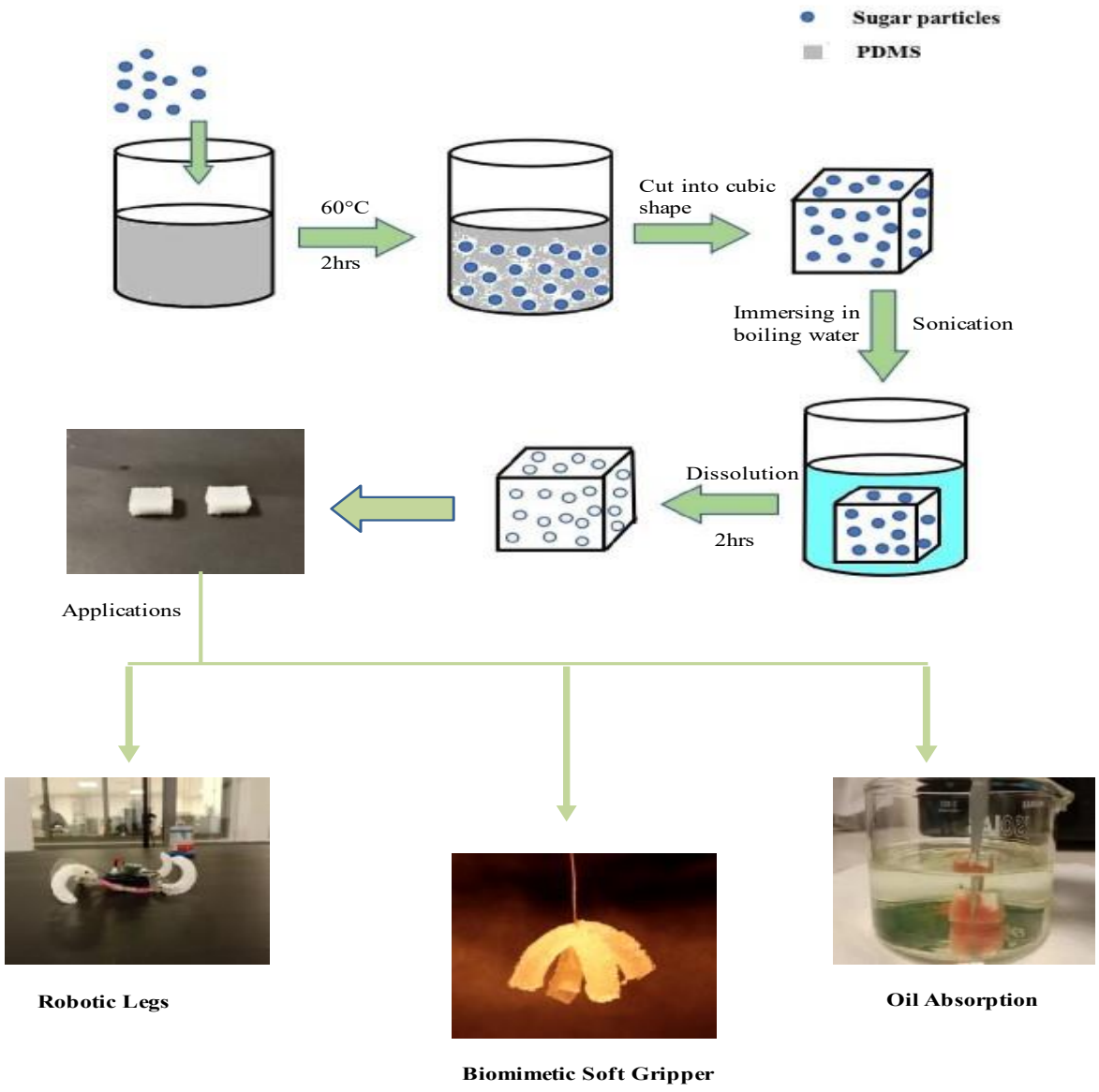

Figure 12: Graphical representation of synthesis and application of PDMS sponges

2.3. Attenuated Total Reflectance (ATR) Spectroscopy Analysis

To see the effect of porogen (sugar) on chemical shifts of peaks for PDMS, the ATR analysis of bulk PDMS, PDMS with sugar, and small sugar PDMS sponge was done. The samples were detected with a resolution of 4.0 cm^{-1} in the 400-4000 cm^{-1} range.

2.4. Scanning Electron Microscopy Analysis

For SEM analysis, samples were coated with Au-Pd using Precision Etching Coating System (PECS^{TM}). Then, these were transferred to an FEI Quanta 200 FEG instrument for the SEM analysis. Voltage 20KV and spot size 5 were used for these measurements. For sugar particle diameter measurements, 15 crystals were selected from each type of sugar.

2.5. Water Contact Angle Measurements

Water contact angle measurements were done to assess the surface wettability of PDMS sponges. For this, the samples were placed on the glass slides and then put on the instrument. The water drops volume of 5 microliters and rate of dropping “medium” was selected. 2 different sets of PDMS sponges were prepared for this analysis. In one set, the concentration of PDMS and Crosslinker was 10:1, and in the other set, it was 5:1.

2.6. Thermogravimetric (TGA) Analysis

The thermogravimetric analysis was done to evaluate the thermal stability of small sugar PDMS sponges. For this 6.5 mg sponge sample was loaded onto the instrument, and the TGA profile of the sample was recorded between 0 and 900 °C.

2.7. Dynamic Mechanical Analysis (DMA)

The Dynamic Mechanical Testing of different PDMS sponges was done to measure the stress/strain behavior, stiffness, and storage modulus. For this disk shape samples were prepared for compression test. All the measurements were taken at 26 °C.

2.8. X-ray Photoelectron Spectroscopy (XPS) Analysis

For XPS, small sugar PDMS sponge samples of different porosity were mounted on copper tapes to increase the conductivity. Thermo Scientific k-alpha XPS instrument using an ion etch with 2000kv was used. XPS spectra of different spots were taken, and elemental analysis was done using instrument software.

Chapter 3

3. Result and Discussion

3.1. Attenuated Total Reflectance (ATR) Spectroscopy Analysis

In order to see the chemical interactions between PDMS and sugar particles, ATR analysis of PDMS, PDMS+ sugar, and PDMS sponge was done. It can be confirmed by the transmittance profile that there was no chemical composition change after this sponge process was done to PDMS as the sugar only created pores in PDMS and was completely removed after this process. The FTIR analysis confirms the presence of characteristic peaks of PDMS in both samples PDMS bulk as well as in PDMS sponge. The peaks around 2905 and 2970cm^{-1} are indicating the symmetric and asymmetric stretching in ≡Si− CH3 of the CH_3 group. Furthermore, the deformation of -CH_3 vibration in PDMS can be easily seen in the peaks of ATR spectra at 1270 and 1400 cm^{-1}. In addition to this peak around 930-1200cm^{-1} are a clear indication of Si-O-Si deformation or stretching. Moreover, the Si-C bands are indicated by the peaks of 850 and 804 cm^{-1}. All of these characteristic peaks can be confirmed from the work of Choong et al[86].

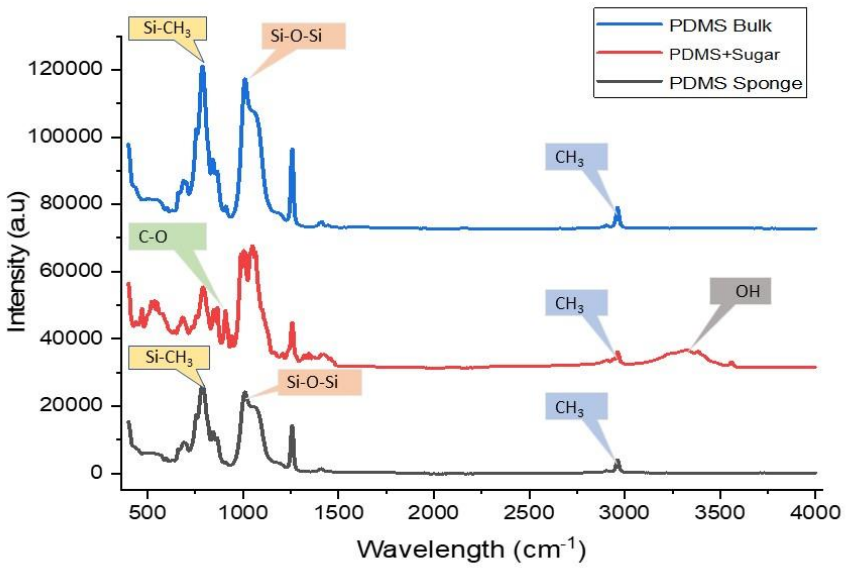

Figure 13. ATR survey of bulk PDMS (blue), PDMS+ sugar (red), and small granules sugar PDMS sponge (black). The PDMS sponge graph shows no -OH peaks, confirming complete removal of sugar from the PDMS sponges.

The ATR spectra of PDMS with sugar is indicating a peak around 3300cm^{-1} which is a clear indication of the -OH group in sugar particles and the disappearance of the -OH peak in the ATR spectra of the PDMS sponge indicates that sugar has been removed after making PDMS porous. The intensity of the peaks in the ATR spectra of the PDMS sponge is decreased a bit compared to the peaks of PDMS bulk due to the formation of pores. Overall, the ATR spectra of PDMS bulk and PDMS sponge remains unchanged in terms of the position of peaks which suggests that sugar has made no change in term of the chemical structure of PDMS. This is the same as the result obtained by the work of Jose et al[87].

3.2. Scanning Electron Microscopy Analysis

In order to have a close-up view for surface morphology, images were taken by Scanning Electron Microscope (SEM). It can be seen in the images that surface have porous structures and size of pores are not consistent with size of sugar particles for a particular sugar particle size. This is due to distinct size of sugar particles in a sample. For the diameter of sugar particles, 15 particles from each sample were taken for the images, and average pore diameter was calculated. For cube sugar, the pore diameter was calculated both for sugar and PDMS sponge. The average diameter for small granules sugar was found to be 490.97 micrometer, while the diameter of small granules sugar sponge was measured around 474.44 micrometer. Similarly, the pore size in cube sugar was around 487.76 micrometer, but the diameter of cube sugar sponge (523.55 micrometer) was not found consistent with pore size in sugar. This can be attributed to the varying size of empty spaces in the cube sugar, which resulted in this disparity of pore diameter. The average diameter of particles in big granules sugar was found 852.07 micrometer, and the diameter of pores in sponge was measured in the range of 830.65 micrometer. The average pore size of sponges was estimated to be somewhat less than the particle size in the sugar, and this can be justified by the brittle nature of sugar. When sugar is mixed with PDMS, due to mixing process, some sugar particles might be broken at edges, but even after this explanation the average pore size is almost same as the particle diameter of sugar particles.

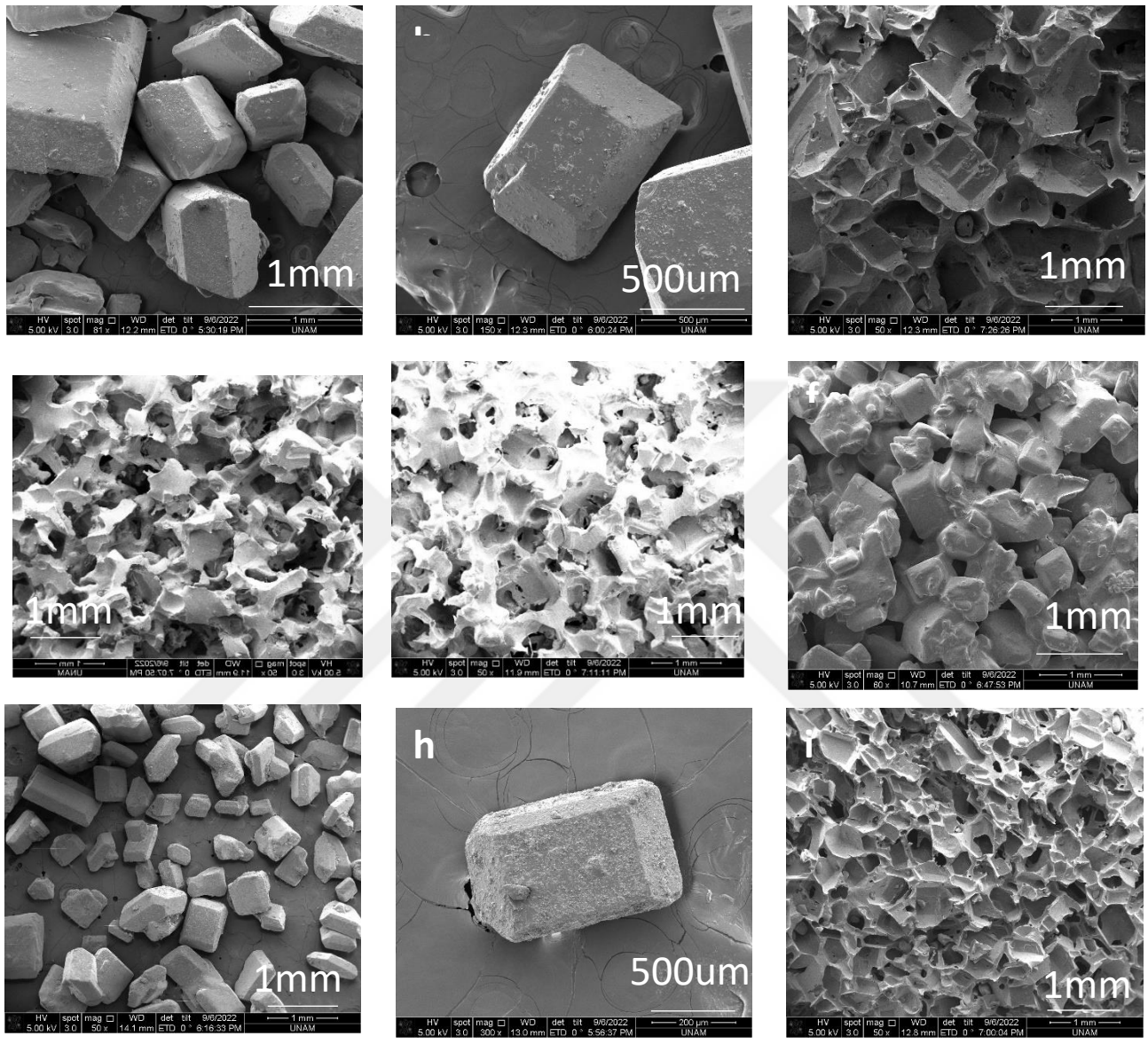

Figure 14: SEM images of (a) big sugar particles, (b) single particle of big sugar, (c) PDMS sponge produced by using big granules sugar, (d) cube sugar pores, (e) cube sugar side, (f) cube sugar sponge, (g) small sugar particles, (h) small granules sugar single particle, (I) small sugar granules sponge.

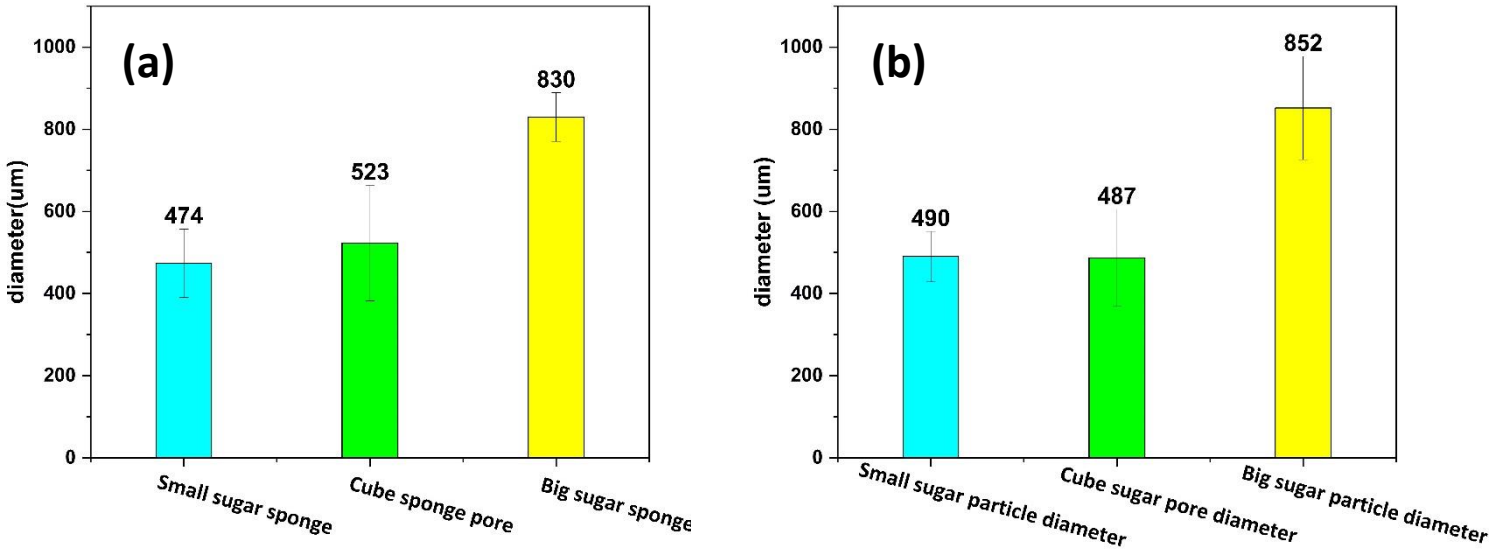

Figure 15: Average diameter of pores in (a) PDMS sponges and (b) sugar particles. The pore size is almost the same as the particle size of sugar used to create the pores.

3.3. Water Contact Angle Measurements

The surface wettability of any material depends upon the chemical composition of material which determines the surface free energy of substances[88]. To achieve maximum absorption capacity of oil/water separation material, the composition must be favorable to interact physically with non-polar components of oil for super-hydrophobicity. The intrinsic hydrophobic nature of PDMS makes it a promising candidate for this application[41]. The CH_3 moieties on siloxane backbone perfectly play the role for hydrophobicity. The wettability of surfaces can be measured by measuring the water contact angles. There are different modes for measuring water contact angle

I.e., sessile drop method, advancing and receding contact angles with the needle method, tilting method, captive bubble method etc.[89]. We measured water contact angle of porous PDMS by sessile drop method. The surface roughness makes it difficult to measure the accurate degree of angle, so we made 6 measurements for each sample and results were recorded with standard deviation.

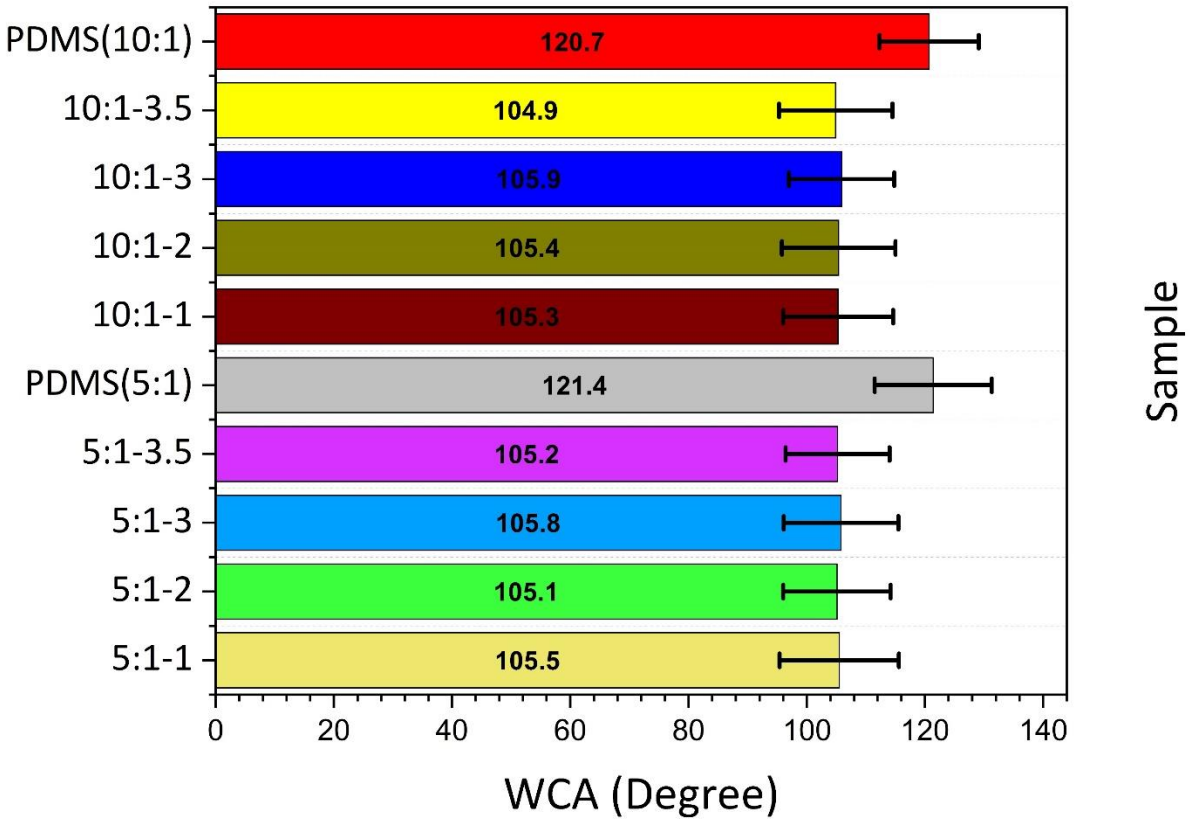

Figure 16: Water contact angle measurements, bulk PDMS (10:1), small granules sugar sponge (10:1-3.5), big granules sugar sponge (10:1-3), cube sugar sponge (10:1-2), bulk PDMS (5:1), small granules sugar sponge (5:1-3.5), big granules sugar sponge (5:1-3), cube sugar sponge (5:1-2).

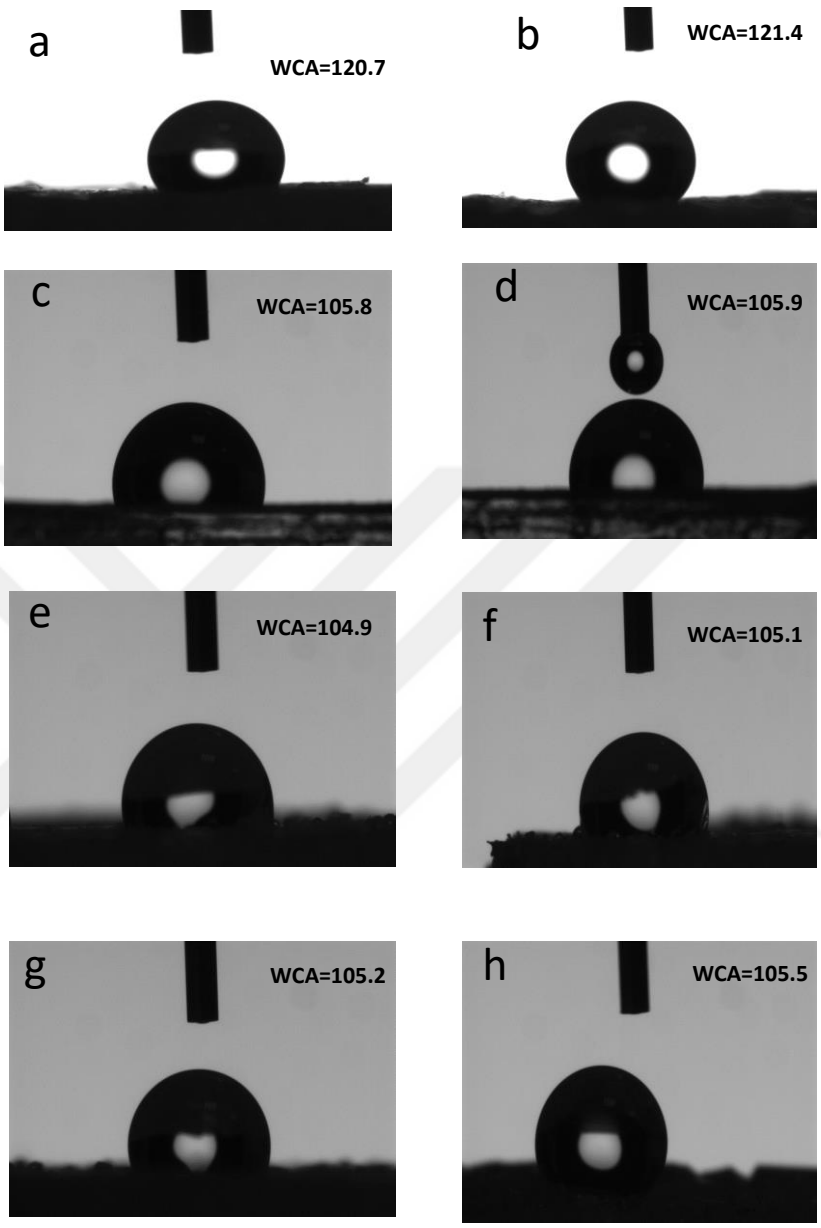

Figure 17: The water contact angle greater than 100 shows that surface of PDMS sponges is hydrophobic. (a) Bulk PDMS (10:1), (b) Bulk PDMS (5:1), (c) big granules sugar sponge, (d) big granules sugar sponge (5:1), (e) small granules sugar sponge, (f) cube sugar sponge, (g) small granules sugar sponge (5:1), (h) mixture of sugar sponge. It is clear from the results that by changing the pore size, there is no effect on the surface wettability, the water contact angle remains almost same.

Typical measurements show that PDMS sponges have contact angles ranging between 97 to 125 degrees with certain standard deviations. 5 uL drop volume was used for all the measurements, and the water contact angle remains almost same with different pore size of samples. This shows hydrophobicity of as prepared material and accounts for selective absorption of oil and organic solvents in the presence of water. In some studies, it has been reported that surface modifications of PDMS with fluorinated silsesquoixanes long chain can dramatically increase the oleophilic characteristic[90][91].

3.4. Thermogravimetric (TGA) Analysis

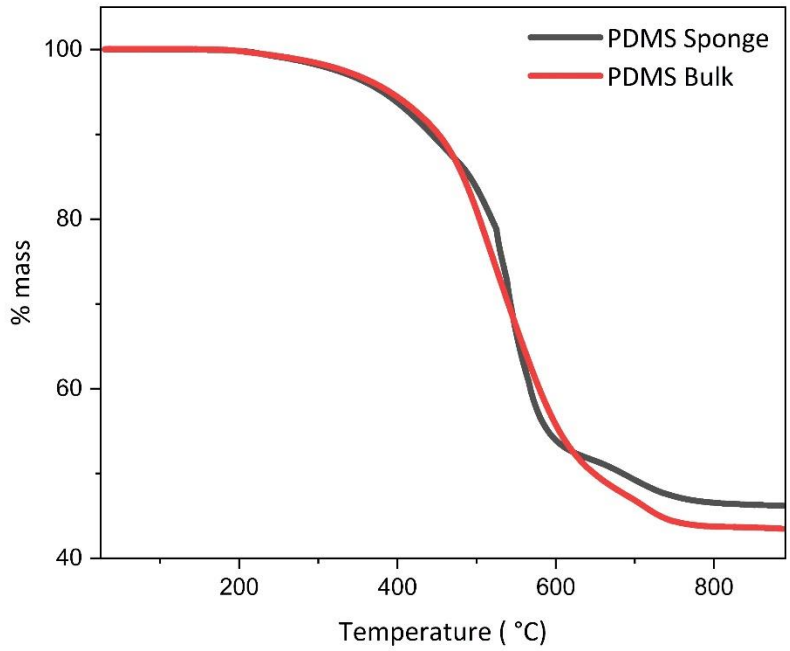

Figure 18: TGA analysis of small sugar PDMS sponge (black) and Bulk PDMS (red). The sponge PDMS is stable up to 350 °C

The Thermogravimetric analysis is showing that bulk PDMS maximally degrades in the temperature range of 300- 900 °C, and it showed a single and sharp mass loss. However, the TGA

of porous PDMS sponge is indicating a broad range of mass loss in the temperature range of 300-700 °C as indicated in the TGA curve of PDMS sponge. In the TGA curve of the PDMS sponge, two overlapping maxima can be easily observed around temperatures 500C° and 620 °C. This data is showing complete relevance to the work of Jose et al[87]. This degradation of PDMS is the result of depolymerization which is accompanied by the residual formation of SiO_2 which is followed by two mechanisms named rearrangement degradation and unzip degradation. In the PDMS polymer chain degradation happens with the breaking bond of Si-O groups. The first degradation curve is around 400-500 °C in the PDMS sponge which indicates the generation of cyclic siloxanes by following unzip degradation mechanism. The peak above than 500 °C indicates the rearrangement degradation of Si-O-Si bonds by heterolytic cleavage. This mechanism is also supported by the work of Laila et al[92].

3.5. Mechanical Testing

The mechanical behaviors of three different sponges i.e., 'small granules' sugar sponge, 'big granules' sugar sponge, and cube sugar sponge were evaluated by Dynamic Mechanical Analyzer (DMA) testing. The disk shape sample were prepared and stress-strain curves for single frequency compression were obtained. It can be seen in the graphs that small granules sugar with more porosity showed greater strain at certain amount of stress, as compared to the others sponges. The cube sugar sponge less strain or compression showing that it has less elasticity. The elastic behavior of all samples can be seen in the graph. The uniaxial strain testing was not found suitable for these sample as sample was broken unevenly before maximum strain was achieved. The Young's Modulus of cube sugar sponge was found to be around 0.95 MPa, while small sugar granules sponge had a Young's Modulus of 0.64 MPa. The big granules sugar sponge has the

elasticity in between these two materials and has a modulus of 0.81 MPa. This was measured by dividing change in volume of sponges in compression test by maximum stress applied at that time.

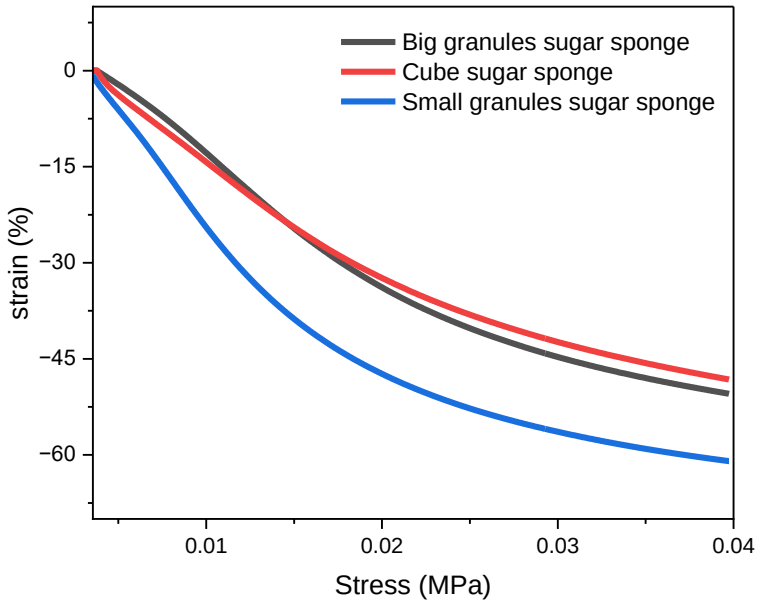

Figure 19: Stress-strain curves for three different sponges i.e., small granules sugar sponge(blue), big granules sugar sponge (black), cube sugar sponge (red)

3.6. X-ray Photoelectron Spectroscopy (XPS) Analysis

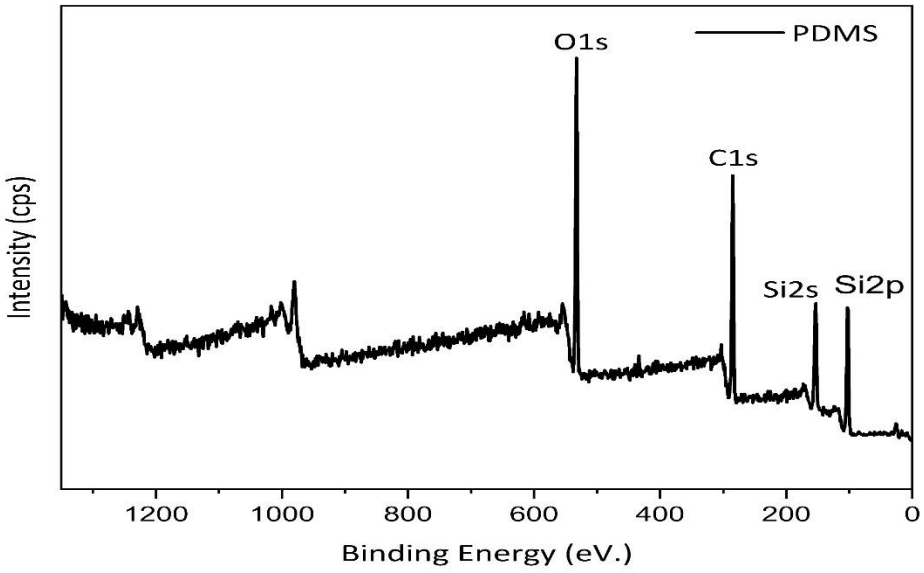

Figure 20: XPS survey of small sugar PDMS sponge

In order to ensure whether sugar particles have made any kind of change in terms of surface energy and structural composition of the PDMS sponge, XPS analysis has been done. Fig.20 which is showing survey scan of XPS of spongy PDMS is depicting the intense peaks of O-1s, C-1s, and Si-2p. These peaks are exactly the same and matchable to the pristine or bulk PDMS, which is a clear indication that sugar cubes have performed no other function except to create pores in PDMS and make it spongy and can be verified by the work of Naushad et al[93] Furthermore, the core spectra of XPS of C-1s depict two peaks that indicate the different connectivity of carbon atom in structure. The peak with higher intensity showed binding energy of 285.08eV and confirmed the existence of the C-H/C-C bond which can be easily anticipated as a CH_3 group in PDMS and the second broad peak appears at 286eV indicates C-O-C bond and it is assumed to appear because of contamination in the air and can also be confirmed from the work of Jhamak et al[94].

Properties	C-1s	O-1s	Si-2p
Peak Binding energy (eV)	285.08	532.94	102.73
Atomic Percentage (%)	45.42%	26.13%	28.45%

Table 2: Binding energies and atomic percentages of C-1s, O-1s, and Si-2p of PDMS sponge prepared with small granules sugar

In addition to this, the core spectra of O-1s indicate the major peak around 532.6eV and confirm the presence of O bridging with Si, another broad peak at 533eV is expected due to the O-C=O which is the possible sign of partial oxidation and this data is relevant to the work performed by Karol et al[95]. Lastly, the core spectra of Si confirm the presence of Si-C and Si-O linkages with the binding energy of 102 eV and 104 eV respectively. Since no new peaks and major peak shift is observed here so it can be inferred that sugar cubes have made no significant interaction with the polymer PDMS sponge and merely created pores and this can be reinforced from the obtained ATR data[96].

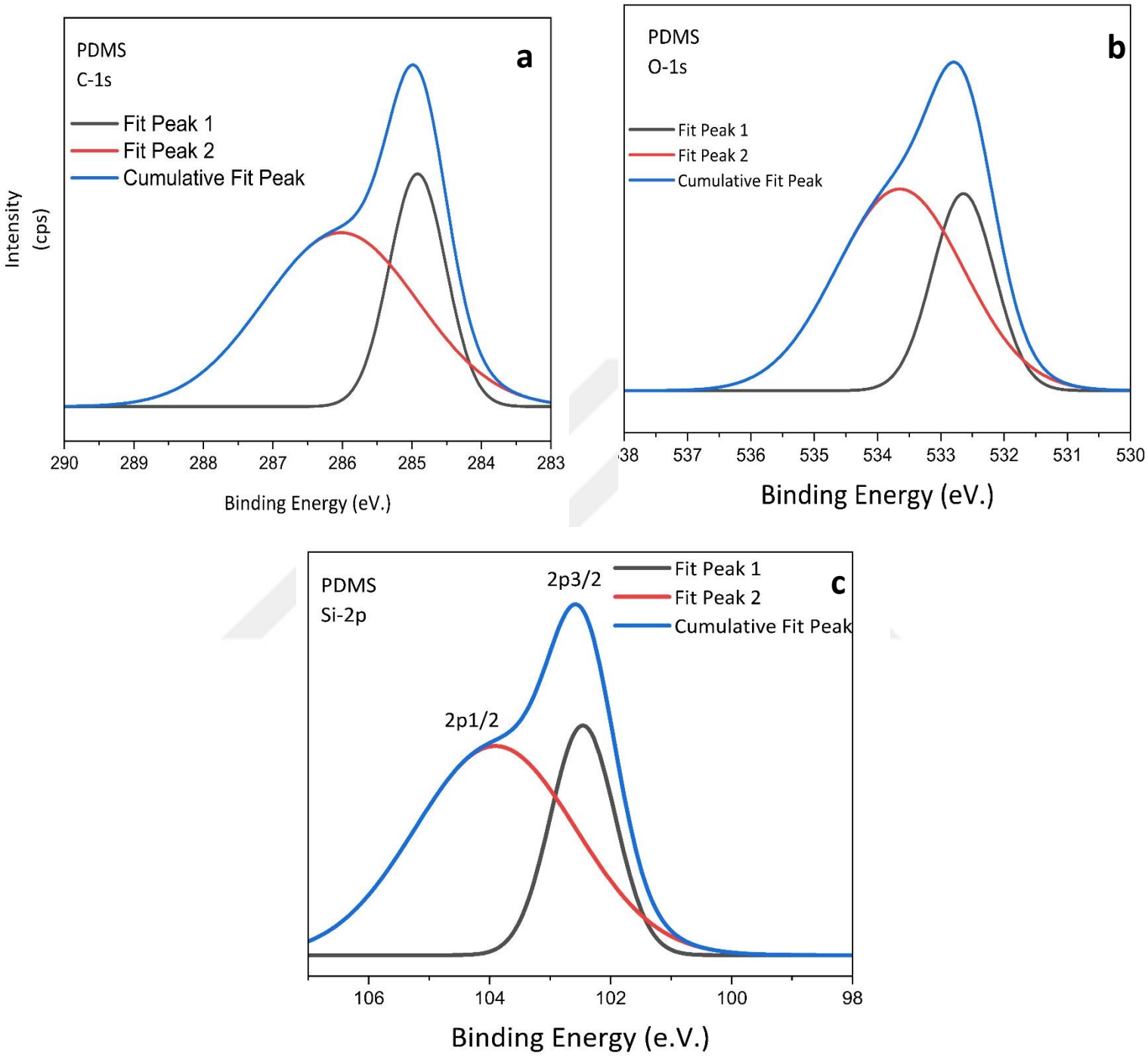

Figure 21: Binding energies (eV.) for C-1s (a), O-1s (b), and Si-2p (c)

3.7. Application of PDMS Sponge for Oil Absorption

Here we demonstrate the use of different PDMS sponges prepared by sugar porogen for separation of oil from water. These sponges were prepared by simple casting fabrication method using sugar particles as porogen to get 3D porous PDMS structure. Casting and molding is an old method to create desired shapes and geometry. The sugar particles in PDMS leave pores and cavities in 3D structure when washed after curing. The porous structure is related to the size of sugar particles and temperature of curing. The melting of sugar available in the market ranges from 160-180 C so the temperature at which PDMS+ sugar mixture is cured is particularly important. The intrinsic hydrophilic nature of PDMS is responsible for high absorption capacity for oils and organic solvents. We used three diverse types of sugar: small granules size, big granules size, and cube sugar. The porosity of all these different sponges solely related to the size of sugar granules. Moreover, the elasticity of PDMS endows the compressibility to the porous structure for squeezing and removing the absorbed oils and organic solvents for many cycles. The ease of fabrication process, and biodegradability of materials make this method facile and environment friendly. The few hours method can produce a large number of materials and is scalable.

3.7.1. Percentage Mass Absorption Capacity

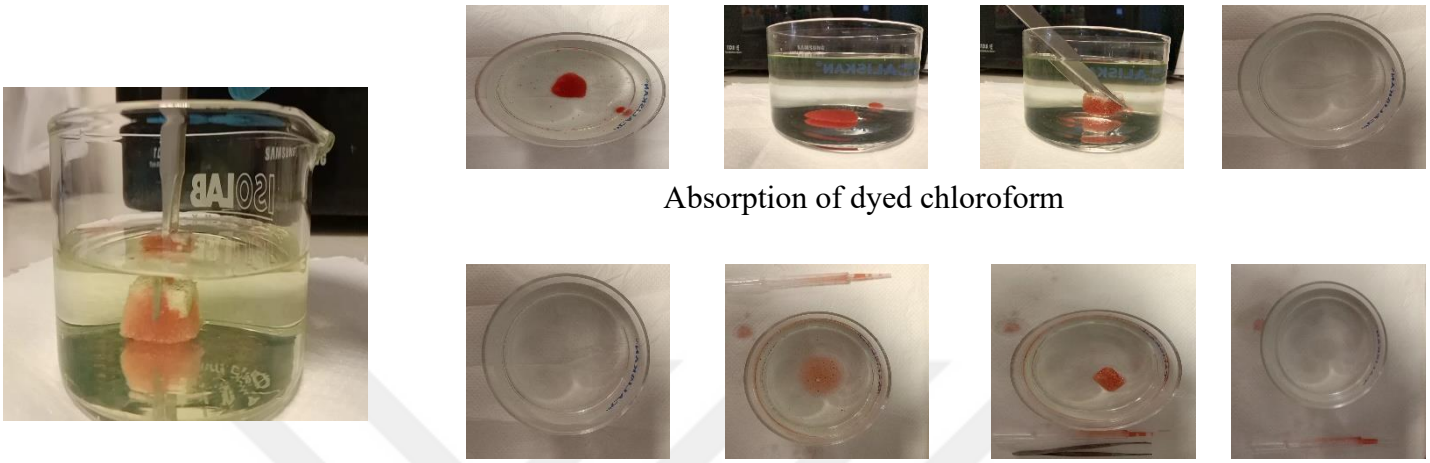

Figure 22: PDMS sponges absorbing the paraffin oil over and under the surface of water. A cube sponge is absorbing chloroform from water under the surface. 3 mL of paraffin oil was added to the water and separation efficiencies were measured for small granules, big granules, and cube sugar sponge.

Various organic solvents (acetone, ethanol, dichloromethane, tetrahydrofuran) and paraffin oil were applied to the PDMS sponges to evaluate their absorption capacities. In this experiment, three different types of PDMS sponges fabricated using various sugars samples were used as a comparison group. Also, the absorption capacity of the bulk PDMS was measured. The mass of all samples was kept same during this experiment to evaluate the exact difference among the absorption capacities of all sponges. Table shows the experimental results according to the internal architecture of the sponges. As shown in the figure 23, the capacities vary for each solvent; this is because the solutions have different densities and solvent compatibilities for PDMS. Of the solvents, dichloromethane absorbed by the small granules sugar sponge gave the largest values observed in the (approximately 800%). With tetrahydrofuran and hexane, the small sugar PDMS

sponges showed an absorption capacity of about 577% and 540% respectively. This pattern of absorption capacities is according to the inner architecture and confirms that the higher the porosity and the more is absorption capacity. Paraffin oil with density around 0.8 g/cm^3 shows the absorption capacity of 183%, 176%, 169% for small granules, big granules, and cube sugar, respectively. Whitesides et al. discussed the swelling of PDMS in different solvents. They concluded that swelling of PDMS in different solvents depends upon the solubility parameter δ of PDMS in that particular solvent. The solubility parameter can be expressed by a sum of the dispersion forces, polar forces, and hydrogen-bonding forces within the material (Hansen's total solubility parameter); that is, $\delta^2 = \delta_d^2 + \delta_p^2 + \delta_h^2$ [82]. On this basis, these solvents can be divided into 3 groups: low solubility solvents, moderate solubility solvents, and high solubility solvents. High solubility solvents such as hexane tend to be non-polar or slightly polar having a dipole moment $\mu \leq 1$ D. The more porosity in small granules sugar sponge and solvent compatibility with hexane is responsible for this maximum absorption capacity.

Material	Density (g/cm3)	Small granules sugar sponge	Big granules sugar sponge	Cube sugar sponge
Water	0.98	15.1 ± 4.23	14.3 ± 5.62	13.7 ± 4.69
Dimethyl sulfoxide	1.1	148.22±3.12	162.63 ± 2.94	146.93± 5.23
Ethanol	0.79	148.77± 3.92	183.93± 5.41	152.41 ± 4.72
Paraffin oil	0.8	183.53± 5.87	176.77± 6.87	169.72± 77
Acetone	0.78	186.61±5.03	201.93± 7.49	245.92± 7.31
n-Hexane	0.66	540.05± 3.98	319.94± 4.82	331.21± 5.5
Tetrahydrofuran	0.88	577.55± 4.15	556.19± 3.65	554.55± 3.87
Dichloromethane	1.33	807.45± 5.6	493.17 ± 4.98	483.03 ± 5.14

Table 3: Density and percentage absorption of different solvents for three sponges.

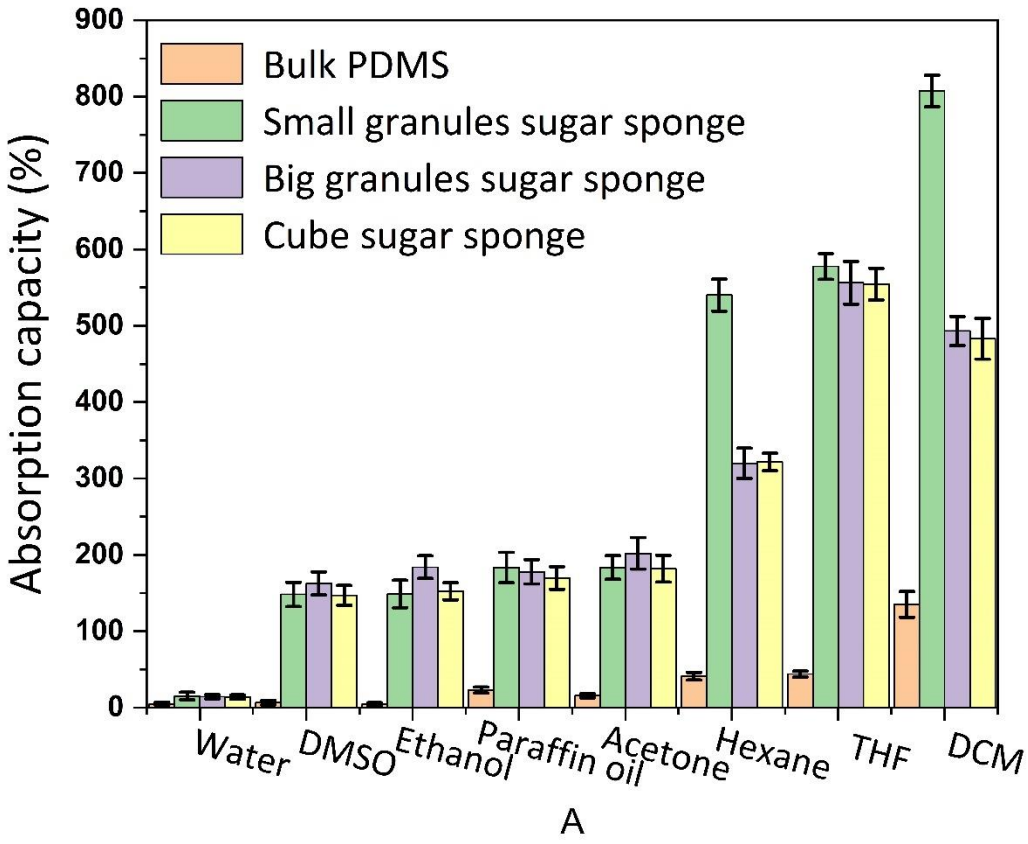

Figure 23: Absorption capacity of bulk PDMS (orange), small granules sugar sponge (green), and big sugar sponge (blue), and cube sugar sponge (yellow). DMSO (Dimethyl sulfoxide), THF (Tetrahydrofuran), DCM (Dichloromethane). The % absorption capacity of sponges depends upon the density of solvents, porosity of sponges, and solvent compatibility for PDMS.

3.7.2. Oil Recovery at different pH Levels

The absorption capacity and separation functionalities of three different sponges for oils were also assessed under different pH conditions to show that these sponges can work effectively in sea (pH is ~8.1) water and fresh water. For this, three water sample with pH 2, 7, and 12 were placed in a beaker, and known weight of paraffin oil was added dropwise. Then, three different sponges were placed on the surface of water to absorb the oil. The percentage of oil absorbed was calculated by the difference of the weight of oil dropped in water and weight of oil absorbed and plotted as graphs. Several measurements were made to obtain the value and the results were recorded. As it can be seen in the figure 24 that all PDMS sponges sample showed almost equal absorbencies. To adjust the particular pH, 1 N NaOH and 1 N HCl solution were added to distilled water until desired pH was reached. The small granules sugar sponge collected almost 92, 91, and 92 % of paraffin oil in water with pH 7, 2, and 12. Similarly, cube sugar sponge and big granules sugar sponge also retained their functionalities under different pH for oil separation. So, these results confirmed the possibilities of PDMS sponges for oil/water separation in different pH environments.

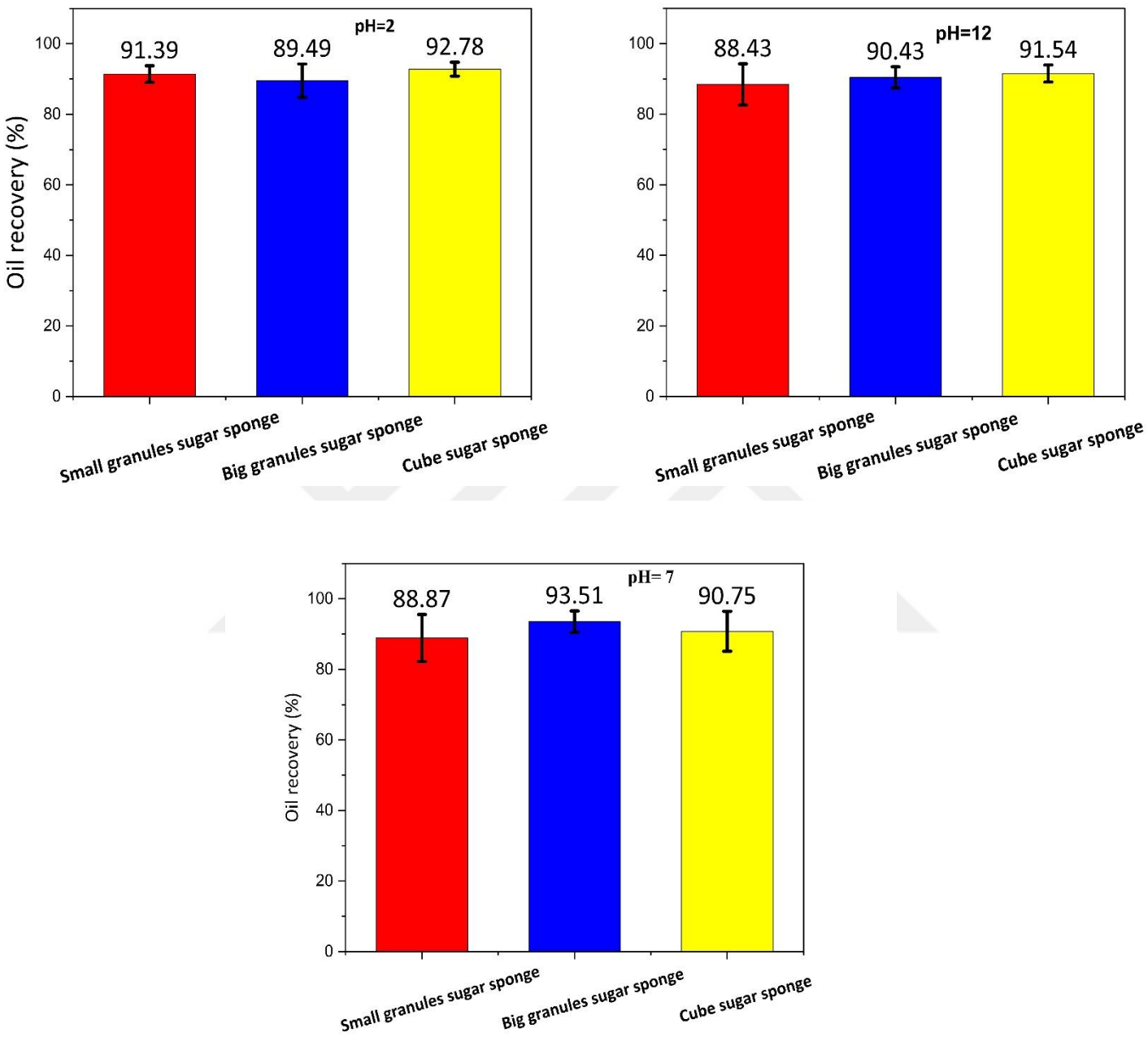

Figure 24: Oil absorption capacity for three different PDMS sponges at different pH (2,7, and 12). Paraffin oil was absorbed with almost same absorption capacity without being affected by pH change. It shows that material can be used for oil/water separation in different pH environments.

3.7.3. Recyclability of Oil Absorption

Recyclability is an important requirement for the practical applications of these sponges for long term use. This aspect of the PDMS sponges was also evaluated by repeating the absorption and desorption of different solvents for different sponges to see the effect of many cycles on absorption capacity. For this assessment, 5 big granules sugar PDMS sponge sample were immersed in acetone solvent and squeezed. The weights of the wet and dry sponges were measured. Before next cycle, the PDMS sponges were washed with ethanol and dried in the oven to make sure no residual solvent is adhered to the sponge. This process was repeated 10 times. As shown in the graph, throughout the iterations, the absorption capacity is well maintained. The same procedure was adopted for cube sugar sponge samples with acetone as solvent for absorption. After 10 cycles of acetone absorption and desorption, a water drop was placed on the PDMS sponges; no absorption of the drop was observed. This indicates that the hydrophobicity and oleophilicity characteristics of the surface were conserved after repeated use.

(a)

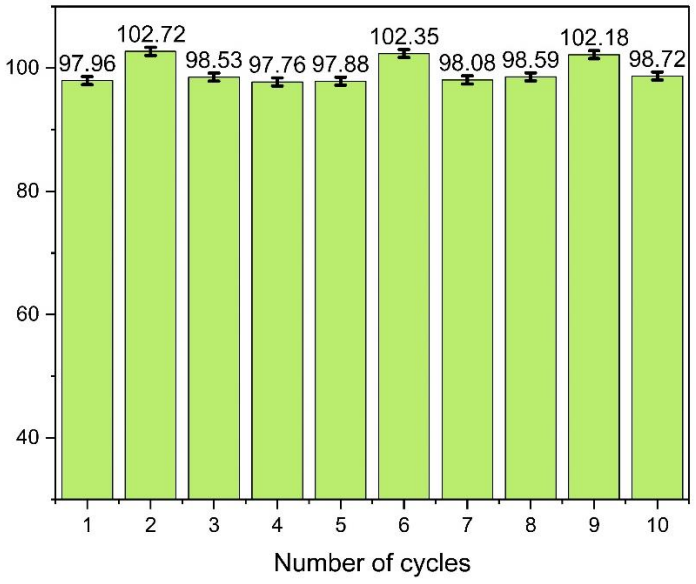

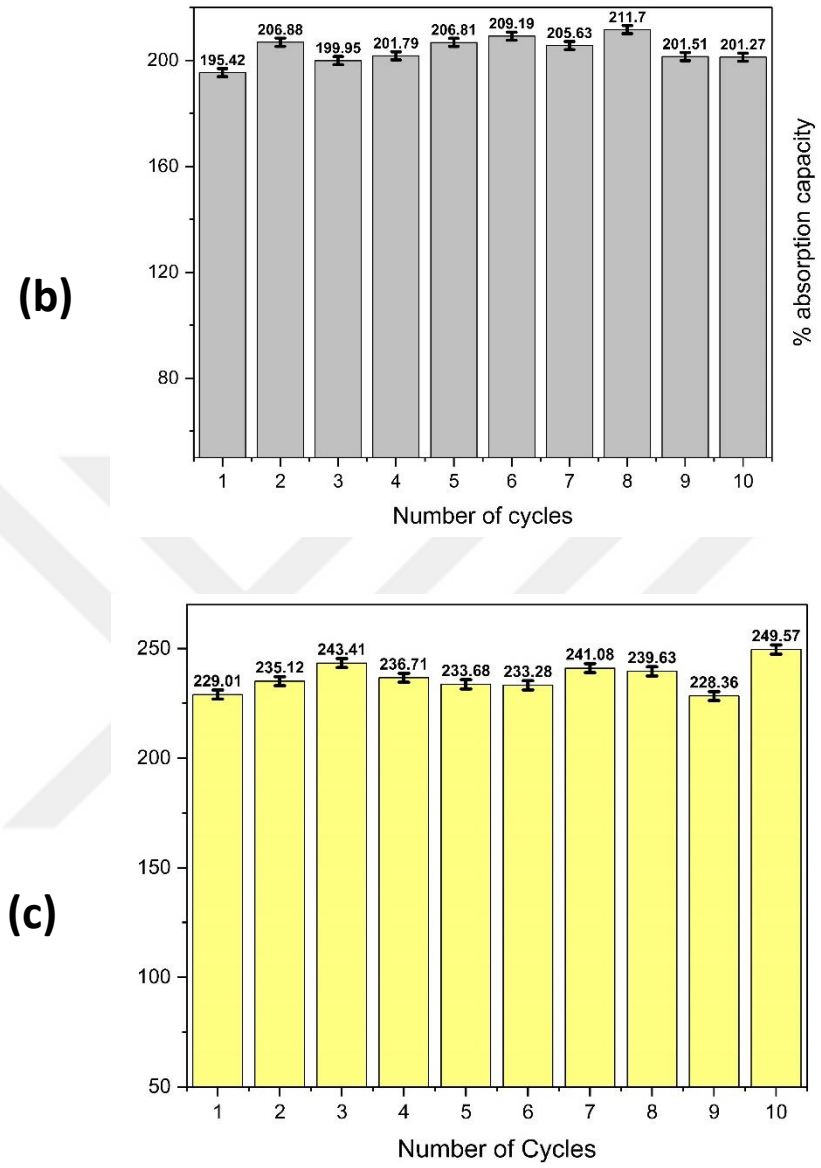

Figure 25: Recyclability of oil absorption for all three sponges (a) big sugar granules sugar sponge, (b) small granules sugar sponge, (c) cube sugar sponge. It is clear from the graphs that the separation efficiency remains almost same after repeated use.

3.7.4. Absorption of Chloroform

Due to its higher density and molecular weight (1.48 g/cm^3), the chloroform, when added to the water, stays under the surface. In order to observe the absorption capability of PDMS sponges to separate high density oil from water under the surface, the red-dyed chloroform was added dropwise to the beaker of water. The PDMS sponges excellently absorbed the maximum of amount of dyed chloroform. This experiment perfectly displayed the application of PDMS sponges for oil absorption under the surface of water.

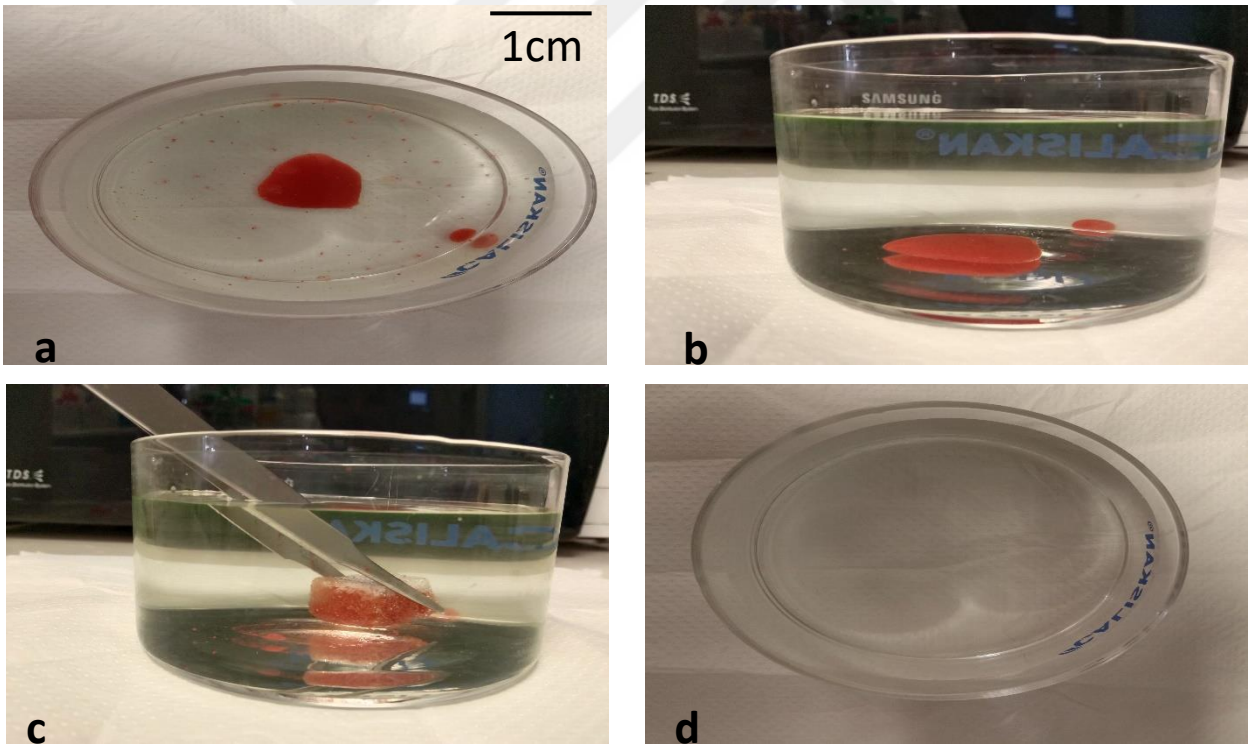

Figure 26: Absorption of chloroform by PDMS sponges. (a) few drops of chloroform were added to the water, (b) due to higher density, chloroform stays on the base of beaker, (c) absorption of chloroform by PDMS sponge, (d) complete absorption by PDMS sponge makes water clean.

3.8. Application of PDMS Sponge as a Biomimetic Soft Gripper

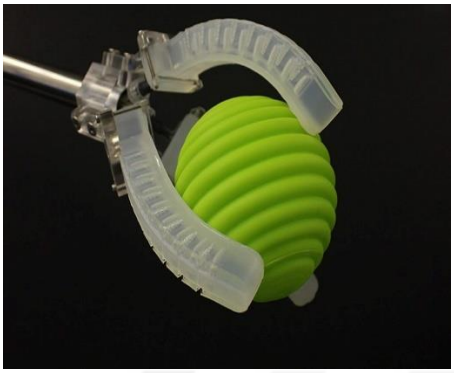

Figure 27: A soft gripper is holding an object. Soft grippers are widely being used in industry to handle delicate objects and picking up fruits for packaging.

One of the most important characteristics of materials used for soft robotics is to respond to the external stimuli. These stimuli i.e., heat, pH, electrical field, magnetic field, chemical environment, etc., induce specific changes in the properties and structure of materials and these changes are exhibited in the form of moving away or towards the source, change in electrical conductance, magnetic properties changes, or change in the shapes and volumes. These deformations like isotropic/anisotropic swelling and variation of stiffness are of great importance for specific actuation. This unique phenomenon of response to an external stimulus can be manipulated for programmable actuation and sensing, unlocking the new possibilities of robotics design with built-in mechanical intelligence and opening new horizons for various new applications[17][16].

As one of the most important intelligent materials, polymeric hydrogel actuators responding to various external stimuli such as heat, pH, light, chemicals, and electricity for controllable and reversible shape transformation have been effectively applied as soft robots artificial muscles, valves, and so on[97]. With the isotropic structures of the hydrogel actuator, only simple

homogeneous swelling/shrinking could be observed under constant stimuli. Still, for complex deformations/movements, the design should be simple but viable.

These principles can also be applied to other polymeric structures for actuation. The current investigated approaches to realize complex deformations/movements can be divided into two main categories: 1) external stimuli can be made non-uniform for a uniform structure and 2) preparation of internal anisotropic structure of polymers with uniform stimuli[98][99]

The application of nonuniform external stimuli onto specific polymeric structure is hard to achieve, therefore, the fabrication of anisotropic structures has been more popular approach to achieve complex deformation. These hydrogel actuators could provide various complex deformations/movements upon uniform stimuli due to the heterogeneous responsiveness of inhomogeneous properties. These anisotropic architectured actuators could provide various complex deformations and movements upon uniform stimuli due to the nonhomogeneous responsiveness of inhomogeneous properties.

It is a universal principle that the structure and properties essentially define the applications of materials. Therefore, the design and fabrication of anisotropic structures is fundamental for the development of chemical stimuli responsive actuators. Bilayer polymeric actuators, consisting of two different polymers sheets with different swelling rates or ratios, have been successfully developed to perform controllable deformations such as bending and bucking on the basis of asymmetrical responsive properties of the two parts. The mismatch swelling or anisotropic responsiveness can be used for actuation and lifting objects as a gripper.

Whitesides *et. al* discussed the solvent compatibility of PDMS for many solvents in microfabrication[82]. It was observed that PDMS swells with different ratios in different solvents.

Experimental measurements of swelling were found to be correlated with the solubility parameter, δ (cal1/2 cm-3/2), which is based on the cohesive energy densities, c (cal/cm3), of the materials. Solvents that swelled PDMS the least included water, nitromethane, dimethyl sulfoxide, ethylene glycol, perfluorotributylamine, perfluoro decalin, acetonitrile, and propylene carbonate; solvents that swelled PDMS the most were diisopropylamino, triethylamine, pentane, and xylenes, hexane, and dichloromethane. This swelling often considered as a negative aspect of PDMS for fabrication purposes, but it can be manipulated for desired swelling with specific degree for actuation and designing a soft gripper[82].

In our design, we have fabricated a bilayer PDMS architecture, in which a layer is spongy PDMS, which has the ability to swell to a greater extent as compared to the other layer, which can be a bulk PDMS, silicones, or a paper layer. The layer which has low swelling ratios in organic solvents as compared to PDMS sponge, can serve as a strain limiting layer and have the ability to bend the bilayer in a specific direction. This directional bending of bilayer structure can be effectively employed to design a biomimetic soft gripper to lift the objects.

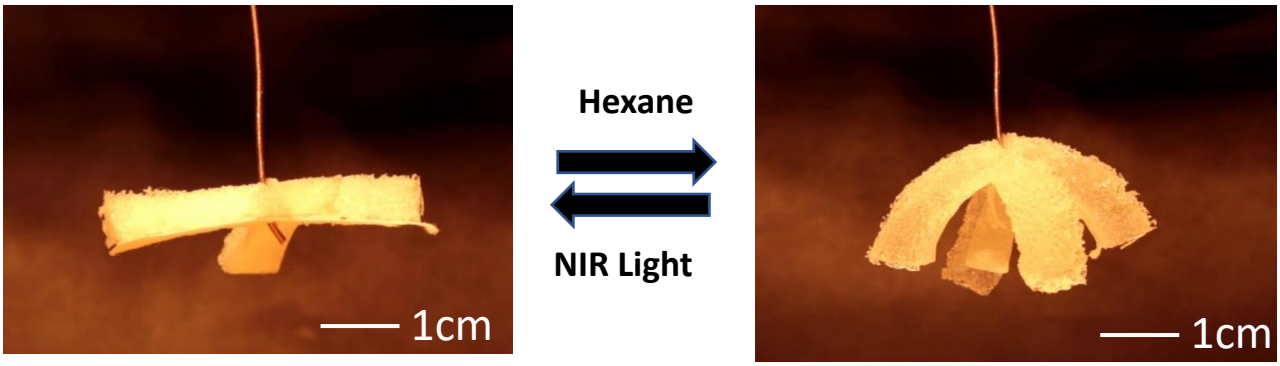

Figure 28: Open claw and close claw shape of the soft gripper in response to NIR light and hexane, respectively.

In order to verify our hypotheses, we used different solvents to see the swelling ratios of bilayer structure, the response time, and bending angle of the bilayer, biomimetic, and soft gripper. The excellent swelling was observed with dichloromethane, n-hexane, and tetrahydrofuran. Still, hexane was chosen as a solvent for further testing because of its low toxicity, no smell, and it is cheaper and inert, commonly used in chromatography.

The swelling of bulk PDMS, sponge PDMS, Ecoflex(silicone), and paper were measured and plotted for comparison. To achieve a better function of the strain limiting layer (the less swelling layer), the difference between the PDMS sponge and the other layer should be maximum to provide greater strength for bending. Henceforth, the paper was stuck on the surface of the PDMS sponge for the fabrication of a soft, biomimetic gripper.

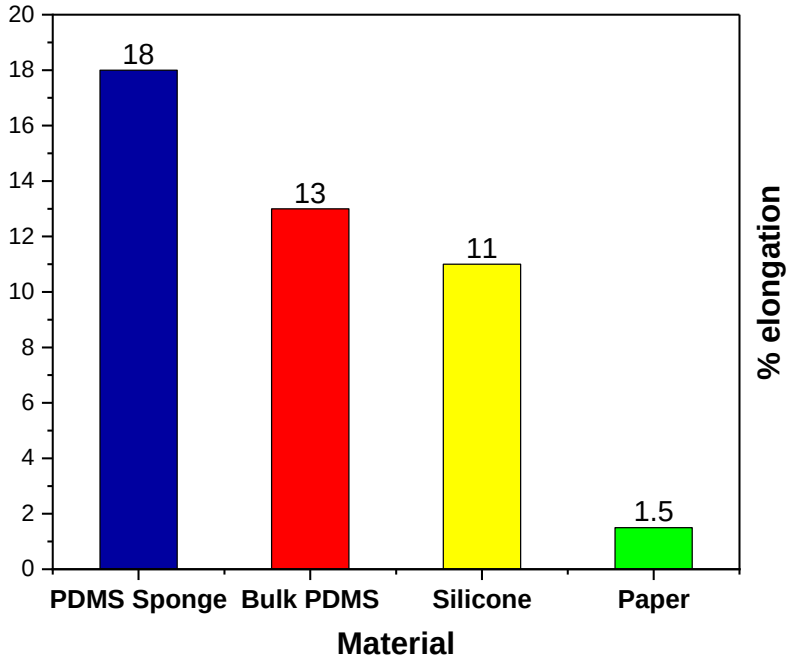

Figure 29: % elongation of different materials in hexane to observe volume change. The greater difference between swelling of PDMS sponge and paper was chosen as a model to fabricate soft gripper.

We measured the swelling of three different sponges in hexane, dichloromethane, and tetrahydrofuran with standard deviation. The sponges with small pore size and maximum porosity, (fabricated by small granules sugar) have higher swelling ratios as compared to the other sponges. This can be verified by looking at the graphs. The swelling in tetrahydrofuran and dichloromethane is though maximum, but due to the bad smell and toxicity issues, it was not used as a solvent for actuation.

$$\% \, Swelling = \frac{li - lo}{li} x100$$

$$l_i = initial\ volume$$

$$l_o = final\ volume$$

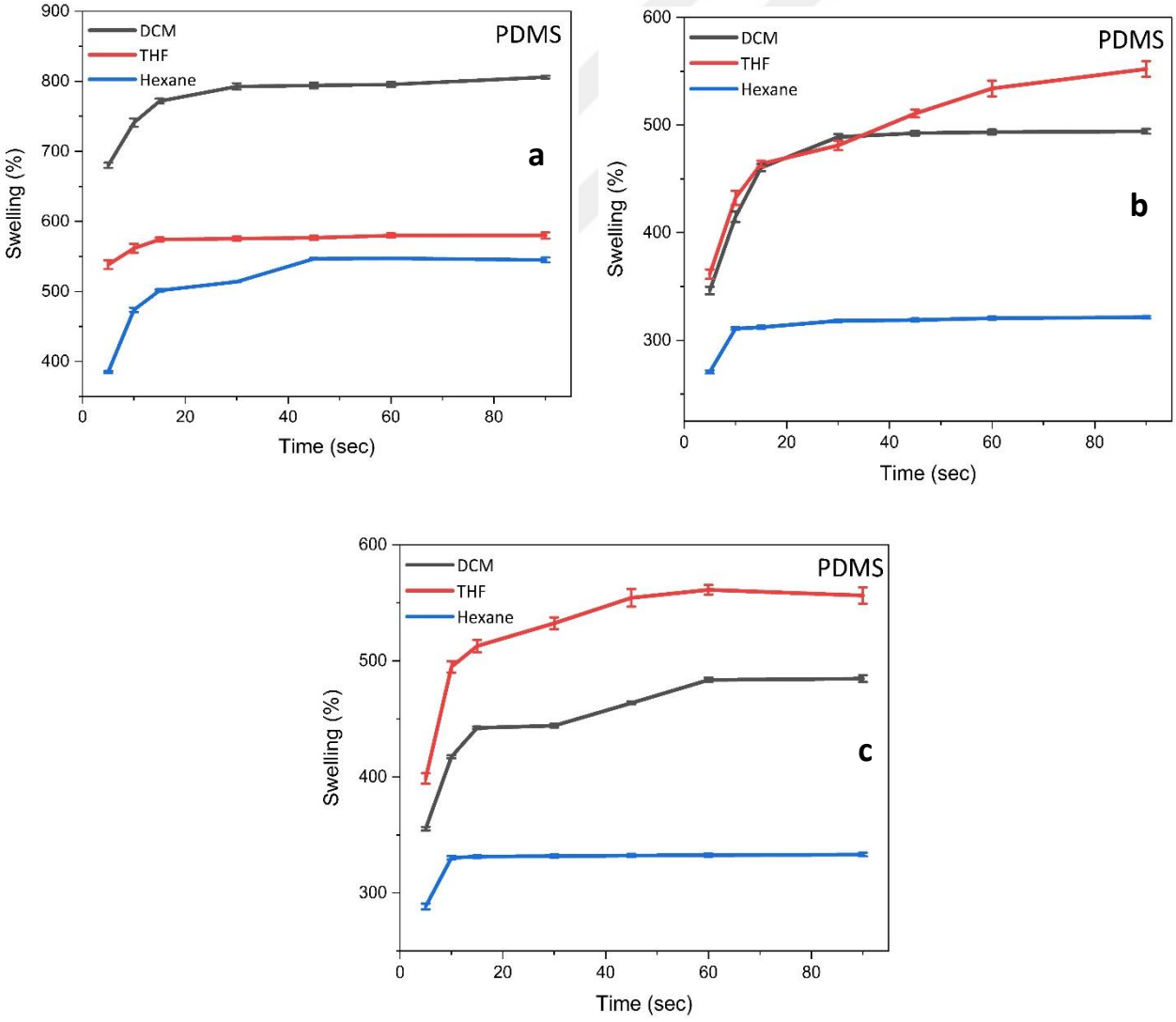

Figure 30: Swelling ratios of (a) small granules sugar sponge, (b) big granules sugar sponge, and (c) cube sugar sponge in dichloromethane, tetrahydrofuran, and hexane. The small sugar sponge has maximum swelling ratio in each solvent.

Although designing actuators to grab a specific object by soft intelligent materials is highly interesting, it is still difficult to design the actuator devices with the ability of multiresponsive complex deformations. Owing to the precisely controllable swelling of bilayer structures in different solvents and complex deformations, our spongy PDMS- paper bilayer gripper can be applied to fabricate a chemoresponsive actuator which can grab an object when dipped in hexane and can release it when irradiated by near infrared light. Due to the heterogeneous swelling, this actuator can reversibly deform from an open-claw shape to close -claw shape to grab and release object, which has the potential as a remote-controllable self-actuator.

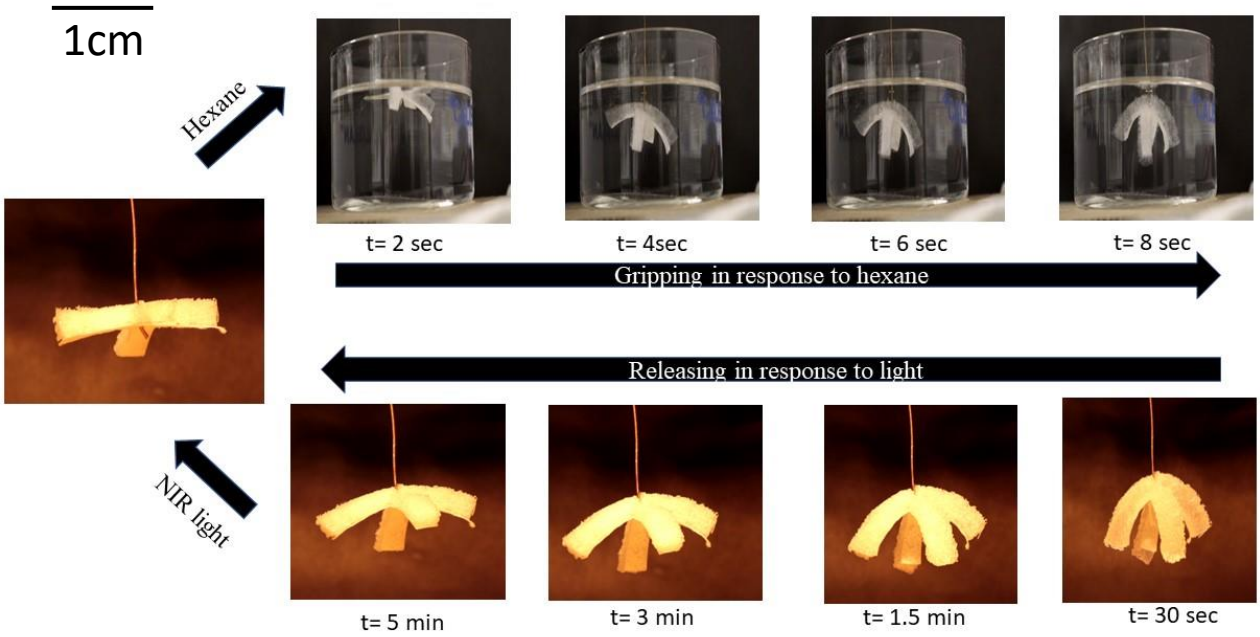

Figure 31: Bending of soft, biomimetic gripper to lift the objects when dipped in hexane solvent. When irradiated under near-infrared light, the claws go in open position to release the objects. The anisotropic swelling of PDMS sponge and paper enables the gripper to show movement in specific direction. The response time to grab the object in hexane solvent is around 8 sec. For releasing object in response to light, it takes approximately 5 minutes to fully evaporate the hexane out of sponges.

In order to observe the response time of soft gripper, the bending angle for grabbing objects in the hexane solvent and releasing objects when irradiated under NIR light was measured. When dipped in the hexane solvent, the gripper deforms to close-claw shape within seconds of time to grab the objects. This can be attributed to the more swelling of spongy PDMS as compared to the paper layer on it. So, paper layer acts as strain limiting layer and fingers of gripper bend in downward direction to attain close-claw position. The low response time for grabbing objects can be justified by the fast diffusion of hexane in spongy material, and excellent solvent compatibility of PDMS for hexane.

To release the object, when NIR lamp was turned on, the response time was calculated up to 5 minutes, which is more than the time for grabbing the objects. The heat increases the rate of evaporation of hexane from the spongy PDMS, and due to the higher solvent compatibility of hexane for PDMS, and vapor pressure of hexane account for this low response time.

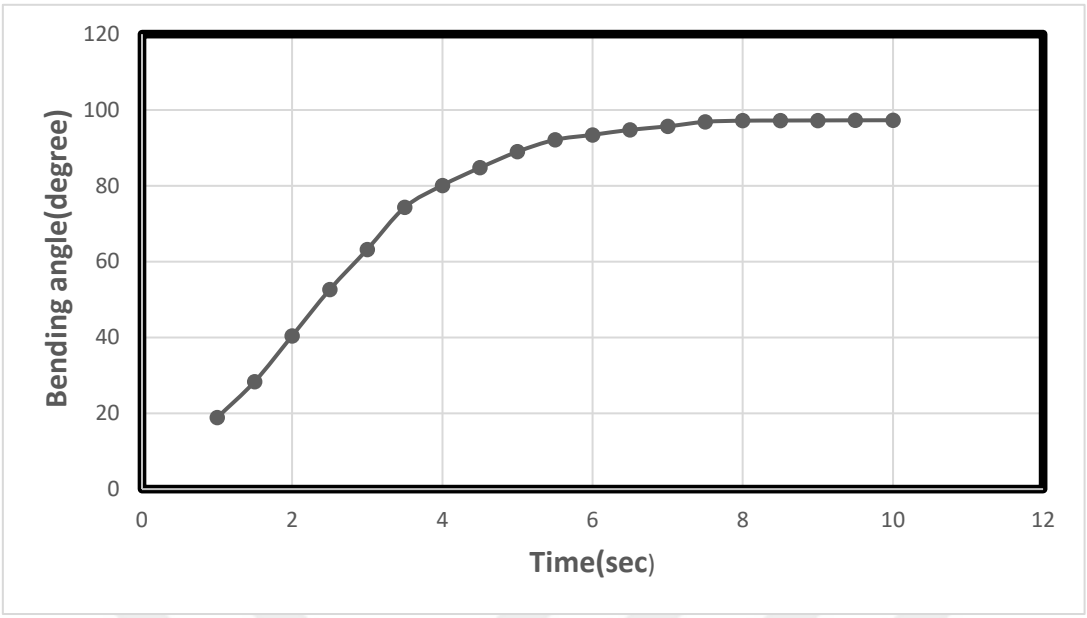

(a)

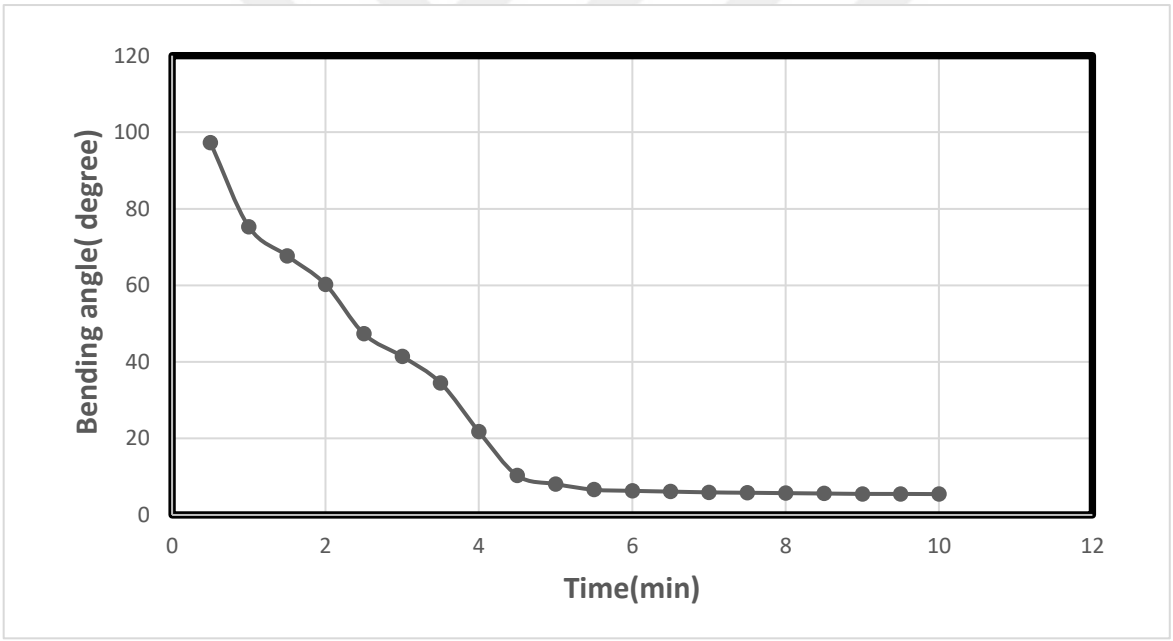

(b)

Figure 32: Measurements of time response for (a) grabbing object (b) release of object in response to NIR light.

4. Conclusion

This work demonstrates the preparation of soft, poroelastic PDMS sponges using sugar as a porogen for pore formation, for soft robotic application. The sugar particles and sugar cubes were used to obtain a 3D porous architecture with different pore sizes and porosity. The pore size and porosity of PDMS sponges depend upon the particle size and concentration of sugar porogen used in different samples. ATR, XPS, and TGA analysis confirm that there is no change in the composition, surface energy, and thermal characteristics of PDMS after porous architecture formation.

In this work, the application of PDMS sponges as a different part of soft robots has been investigated. This achievement not only cut short the power consumption of robots but also endows more flexibility and elasticity to the body of soft robots for performing different tasks in an unstructured environment. Another interesting application of this spongy PDMS material was the separation of oil from the wastewater was also demonstrated. The mass absorption capacity of PDMS spongy material was calculated for various organic solvents and oils, and it is concluded that spongy PDMS can be effectively employed for the treatment of oil spills in all kinds of water bodies. Recyclability of oil absorption- desorption and retainment of oil absorption capacity at different pH levels evidently displays the application of this PDMS spongy material for oil-water separation in different conditions, and this material can be effectively used as a part of the swimming robots to be deployed in remote areas for this purpose.

In the final part, this PDMS spongy material has been used to design a soft, biomimetic spongy gripper that can lift/ grab the objects in the presence of a chemical stimulus (hexane) and release the object in response to near-infrared light. The anisotropic swelling of bulk PDMS and PDMS

sponges in different solvents provided the basis for this system design. It was noticed that the combination of two different layers, with different swelling ratios in a solvent, can be excellently manipulated to fabricate a stimuli-responsive soft gripper to grab the objects in a controlled fashion. The irradiation of the bilayer structure under NIR light accelerates the evaporation of the solvent (hexane) and facilitates the bilayer structure to regain its shape and release objects. This stimuli-responsive system doesn't require any power source to operate and can be effectively used in industries to pick delicate objects for various purposes.

In future prospects, this work can be further optimized to evaluate the mechanical properties of PDMS sponges prepared by changing the curing temperature and crosslinking concentrations. The oil/water separation capacities of different sponges can also be investigated at different temperatures to ascertain that this material can be effectively used in different environmental conditions. The soft, biomimetic gripper can be further modified to operate without dipping in the solvent with some external pump system to inject hexane and draw it back after the operation is done.

5. References

[1] V. R. Barrientos, J. R. García Sánchez, and R. Silva Ortigoza, "Robots Móviles: Evolución y Estado del Arte," *Polibits*, vol. 35, 2007, doi: 10.17562/pb-35-3.

[2] N. Schurr, P. Varakantham, E. Bowring, M. Tambe, and B. Grosz, "Asimovian multiagents: Applying laws of robotics to teams of humans and agents," in *Lecture Notes in Computer Science (including subseries Lecture Notes in Artificial Intelligence and Lecture Notes in Bioinformatics)*, 2007, vol. 4411 LNAI. doi: 10.1007/978-3-540-71956-4_3.

[3] N. G. Hockstein, C. G. Gourin, R. A. Faust, and D. J. Terris, "A history of robots: From science fiction to surgical robotics," in *Journal of Robotic Surgery*, 2007, vol. 1, no. 2. doi: 10.1007/s11701-007-0021-2.

[4] R. Szabolcsi, "The birth of the term robot," *Adv. Mil. Technol.*, vol. 9, no. 1, 2014.

[5] W. Zhang, A. Dai, and Y. Rong, "Engineering design for robot aesthetics," in *Proceedings of the ASME Design Engineering Technical Conference*, 2015, vol. 1B-2015. doi: 10.1115/DETC2015-47218.

[6] M. Mariappan, M. Nadarajan, R. R. Porle, N. Parimon, and W. L. Khong, "Towards real-time visual biometric authentication using human face for healthcare telepresence mobile robots," *J. Telecommun. Electron. Comput. Eng.*, vol. 8, no. 11, 2016.

[7] C. P. Baldé *et al.*, *The global e-waste monitor 2017 : quantities, flows, and resources*.

[8] S. Kim, C. Laschi, and B. Trimmer, "Soft robotics: A bioinspired evolution in robotics," *Trends in Biotechnology*, vol. 31, no. 5. 2013. doi: 10.1016/j.tibtech.2013.03.002.

[9] S. Coyle, C. Majidi, P. LeDuc, and K. J. Hsia, "Bio-inspired soft robotics: Material

selection, actuation, and design," *Extreme Mechanics Letters*, vol. 22. 2018. doi: 10.1016/j.eml.2018.05.003.

[10] D. Rus and M. T. Tolley, "Design, fabrication and control of soft robots," *Nature*, vol. 521, no. 7553. 2015. doi: 10.1038/nature14543.

[11] D. Trivedi, C. D. Rahn, W. M. Kier, and I. D. Walker, "Soft robotics: Biological inspiration, state of the art, and future research," *Appl. Bionics Biomech.*, vol. 5, no. 3, 2008, doi: 10.1080/11762320802557865.

[12] C. Majidi, "Soft Robotics: A Perspective - Current Trends and Prospects for the Future," *Soft Robotics*, vol. 1, no. 1. 2014. doi: 10.1089/soro.2013.0001.

[13] J. Shintake, V. Cacucciolo, D. Floreano, and H. Shea, "Soft Robotic Grippers," *Advanced Materials*, vol. 30, no. 29. 2018. doi: 10.1002/adma.201707035.

[14] J. C. Yang, J. Mun, S. Y. Kwon, S. Park, Z. Bao, and S. Park, "Electronic Skin: Recent Progress and Future Prospects for Skin-Attachable Devices for Health Monitoring, Robotics, and Prosthetics," *Advanced Materials*, vol. 31, no. 48. 2019. doi: 10.1002/adma.201904765.

[15] S. I. Rich, R. J. Wood, and C. Majidi, "Untethered soft robotics," *Nature Electronics*, vol. 1, no. 2. 2018. doi: 10.1038/s41928-018-0024-1.

[16] J. Liu, Y. Gao, Y. J. Lee, and S. Yang, "Responsive and Foldable Soft Materials," *Trends in Chemistry*, vol. 2, no. 2. 2020. doi: 10.1016/j.trechm.2019.11.003.

[17] J. M. McCracken, B. R. Donovan, and T. J. White, "Materials as Machines," *Advanced Materials*, vol. 32, no. 20. 2020. doi: 10.1002/adma.201906564.

[18] G. Y. Gu, J. Zhu, L. M. Zhu, and X. Zhu, “A survey on dielectric elastomer actuators for soft robots,” *Bioinspiration and Biomimetics*, vol. 12, no. 1. 2017. doi: 10.1088/1748-3190/12/1/011003.

[19] A. Lendlein and O. E. C. Gould, “Reprogrammable recovery and actuation behaviour of shape-memory polymers,” *Nature Reviews Materials*, vol. 4, no. 2. 2019. doi: 10.1038/s41578-018-0078-8.

[20] T. J. White and D. J. Broer, “Programmable and adaptive mechanics with liquid crystal polymer networks and elastomers,” *Nature Materials*, vol. 14, no. 11. 2015. doi: 10.1038/nmat4433.

[21] X. Liu, J. Liu, S. Lin, and X. Zhao, “Hydrogel machines,” *Materials Today*, vol. 36. 2020. doi: 10.1016/j.mattod.2019.12.026.

[22] Y. Kim, G. A. Parada, S. Liu, and X. Zhao, “Ferromagnetic soft continuum robots,” *Sci. Robot.*, vol. 4, no. 33, 2019, doi: 10.1126/SCIROBOTICS.AAX7329.

[23] Z. Shen, F. Chen, X. Zhu, K. T. Yong, and G. Gu, “Stimuli-responsive functional materials for soft robotics,” *J. Mater. Chem. B*, vol. 8, no. 39, pp. 8972–8991, 2020, doi: 10.1039/d0tb01585g.

[24] Y. Shang, J. Wang, T. Ikeda, and L. Jiang, “Bio-inspired liquid crystal actuator materials,” *Journal of Materials Chemistry C*, vol. 7, no. 12. 2019. doi: 10.1039/c9tc00107g.

[25] C. Yang and Z. Suo, “Hydrogel ionotronics,” *Nature Reviews Materials*, vol. 3, no. 6. 2018. doi: 10.1038/s41578-018-0018-7.

[26] E. Yilgör and I. Yilgör, “Silicone containing copolymers: Synthesis, properties and

applications," *Progress in Polymer Science*, vol. 39, no. 6. 2014. doi: 10.1016/j.progpolymsci.2013.11.003.

[27] C. Eaborn, "Chemistry and technology of silicones," *J. Organomet. Chem.*, vol. 17, no. 2, 1969, doi: 10.1016/s0022-328x(00)88630-1.

[28] Q. Alkhalaf, S. Pande, and R. R. Palkar, "Review of polydimethylsiloxane (pdms) as a material for additive manufacturing," 2021. doi: 10.1007/978-981-15-6619-6_28.

[29] M. P. Wolf, G. B. Salieb-Beugelaar, and P. Hunziker, "PDMS with designer functionalities—Properties, modifications strategies, and applications," *Progress in Polymer Science*, vol. 83. 2018. doi: 10.1016/j.progpolymsci.2018.06.001.

[30] E. K. Sackmann, A. L. Fulton, and D. J. Beebe, "The present and future role of microfluidics in biomedical research," *Nature*, vol. 507, no. 7491. 2014. doi: 10.1038/nature13118.

[31] S. Halldorsson, E. Lucumi, R. Gómez-Sjöberg, and R. M. T. Fleming, "Advantages and challenges of microfluidic cell culture in polydimethylsiloxane devices," *Biosensors and Bioelectronics*, vol. 63. 2015. doi: 10.1016/j.bios.2014.07.029.

[32] J. E. Mark, "Some interesting things about polysiloxanes," *Acc. Chem. Res.*, vol. 37, no. 12, 2004, doi: 10.1021/ar030279z.

[33] J. C. Lötters, W. Olthuis, P. H. Veltink, and P. Bergveld, "The mechanical properties of the rubber elastic polymer polydimethylsiloxane for sensor applications," *J. Micromechanics Microengineering*, vol. 7, no. 3, 1997, doi: 10.1088/0960-1317/7/3/017.

[34] N. E. Stankova *et al.*, "Optical properties of polydimethylsiloxane (PDMS) during nanosecond laser processing," *Appl. Surf. Sci.*, vol. 374, 2016, doi:

10.1016/j.apsusc.2015.10.016.

[35] D. K. Cai, A. Neyer, R. Kuckuk, and H. M. Heise, “Optical absorption in transparent PDMS materials applied for multimode waveguides fabrication,” *Opt. Mater. (Amst).*, vol. 30, no. 7, 2008, doi: 10.1016/j.optmat.2007.05.041.

[36] K. Shimizu, T. Nagai, and J. Shintake, “Dielectric elastomer fiber actuators with aqueous electrode,” *Polymers (Basel).*, vol. 13, no. 24, 2021, doi: 10.3390/polym13244310.

[37] E. Berthier, E. W. K. Young, and D. Beebe, “Engineers are from PDMS-land, biologists are from polystyrenia,” *Lab on a Chip*, vol. 12, no. 7. 2012. doi: 10.1039/c2lc20982a.

[38] S. H. Yun *et al.*, “Characterization and resolution of evaporation-mediated osmolality shifts that constrain microfluidic cell culture in poly(dimethylsiloxane) devices,” *Anal. Chem.*, vol. 79, no. 3, 2007, doi: 10.1021/ac061990v.

[39] H. Shiku *et al.*, “Oxygen permeability of surface-modified poly(dimethylsiloxane) characterized by scanning electrochemical microscopy,” *Chem. Lett.*, vol. 35, no. 2, 2006, doi: 10.1246/cl.2006.234.

[40] A. J. Mäki, M. Peltokangas, J. Kreutzer, S. Auvinen, and P. Kallio, “Modeling carbon dioxide transport in PDMS-based microfluidic cell culture devices,” *Chem. Eng. Sci.*, vol. 137, 2015, doi: 10.1016/j.ces.2015.06.065.

[41] D. Zhu, S. Handschuh-Wang, and X. Zhou, “Recent progress in fabrication and application of polydimethylsiloxane sponges,” *Journal of Materials Chemistry A*, vol. 5, no. 32. 2017. doi: 10.1039/c7ta04577h.

[42] M. Peng *et al.*, “Synthesis and application of modified commercial sponges for oil-water

separation," *Chemical Engineering Journal*, vol. 373. 2019. doi: 10.1016/j.cej.2019.05.013.

[43] S. Liang *et al.*, "3D Stretchable, Compressible, and Highly Conductive Metal-Coated Polydimethylsiloxane Sponges," *Adv. Mater. Technol.*, vol. 1, no. 7, 2016, doi: 10.1002/admt.201600117.

[44] P. K. Yuen, H. Su, V. N. Goral, and K. A. Fink, "Three-dimensional interconnected microporous poly(dimethylsiloxane) microfluidic devices," *Lab Chip*, vol. 11, no. 8, 2011, doi: 10.1039/c0lc00660b.

[45] A. Giustiniani, P. Guégan, M. Marchand, C. Poulard, and W. Drenckhan, "Generation of Silicone Poly-HIPEs with Controlled Pore Sizes via Reactive Emulsion Stabilization," *Macromol. Rapid Commun.*, vol. 37, no. 18, 2016, doi: 10.1002/marc.201600281.

[46] J. Yu, X. Yufeng, L. Xuequan, and S. Li-Hua, "Dual-stimuli responsive carbon nanotube Sponge-PDMS amphibious actuator," *Nanomaterials*, vol. 9, no. 12, 2019, doi: 10.3390/nano9121704.

[47] L. W. Lo, J. Zhao, H. Wan, Y. Wang, S. Chakrabartty, and C. Wang, "A Soft Sponge Sensor for Multimodal Sensing and Distinguishing of Pressure, Strain, and Temperature," *ACS Appl. Mater. Interfaces*, vol. 14, no. 7, 2022, doi: 10.1021/acsami.1c21003.

[48] X. Zhao, F. Meng, and Y. Peng, "Flexible and highly pressure-sensitive ternary composites-wrapped polydimethylsiloxane sponge based on synergy of multi-dimensional components," *Compos. Part B Eng.*, vol. 229, 2022, doi: 10.1016/j.compositesb.2021.109466.

[49] B. C. Mac Murray *et al.*, "Poroelastic Foams for Simple Fabrication of Complex Soft

Robots," *Adv. Mater.*, vol. 27, no. 41, pp. 6334–6340, Nov. 2015, doi: 10.1002/ADMA.201503464.

[50] E. Brauns, "Towards a worldwide sustainable and simultaneous large-scale production of renewable energy and potable water through salinity gradient power by combining reversed electrodialysis and solar power?," *Desalination*, vol. 219, no. 1–3, 2008, doi: 10.1016/j.desal.2007.04.056.

[51] M. Schrope, "Oil spill: Deep wounds," *Nature*, vol. 472, no. 7342. 2011. doi: 10.1038/472152a.

[52] A. A. Al-Majed, A. R. Adebayo, and M. E. Hossain, "A sustainable approach to controlling oil spills," *Journal of Environmental Management*, vol. 113. 2012. doi: 10.1016/j.jenvman.2012.07.034.

[53] D. Chandler, "Interfaces and the driving force of hydrophobic assembly," *Nature*, vol. 437, no. 7059. 2005. doi: 10.1038/nature04162.

[54] S. A. Zengel, J. Michel, and J. A. Dahlin, "Environmental effects of in situ burning of oil spills in inland and upland habitats," *Spill Sci. Technol. Bull.*, vol. 8, no. 4, 2003, doi: 10.1016/S1353-2561(03)00051-3.

[55] R. C. Prince, "Oil spill dispersants: Boon or bane?," *Environ. Sci. Technol.*, vol. 49, no. 11, 2015, doi: 10.1021/acs.est.5b00961.

[56] C. Nam *et al.*, "Practical Oil Spill Recovery by a Combination of Polyolefin Absorbent and Mechanical Skimmer," *ACS Sustain. Chem. Eng.*, vol. 6, no. 9, 2018, doi: 10.1021/acssuschemeng.8b02322.

[57] J. Ge, H. Y. Zhao, H. W. Zhu, J. Huang, L. A. Shi, and S. H. Yu, “Advanced Sorbents for Oil-Spill Cleanup: Recent Advances and Future Perspectives,” *Advanced Materials*, vol. 28, no. 47. 2016. doi: 10.1002/adma.201601812.

[58] V. Broje and A. A. Keller, “Effect of operational parameters on the recovery rate of an oleophilic drum skimmer,” *J. Hazard. Mater.*, vol. 148, no. 1–2, 2007, doi: 10.1016/j.jhazmat.2007.02.017.

[59] L. Li, B. Li, H. Sun, and J. Zhang, “Compressible and conductive carbon aerogels from waste paper with exceptional performance for oil/water separation,” *J. Mater. Chem. A*, vol. 5, no. 28, 2017, doi: 10.1039/c7ta03511j.

[60] B. Liu, L. Zhang, H. Wang, and Z. Bian, “Preparation of MCC/MC Silica Sponge and Its Oil/Water Separation Apparatus Application,” *Ind. Eng. Chem. Res.*, vol. 56, no. 20, 2017, doi: 10.1021/acs.iecr.6b04854.

[61] Z. wei S. Zeng and S. E. Taylor, “Facile preparation of superhydrophobic melamine sponge for efficient underwater oil-water separation,” *Sep. Purif. Technol.*, vol. 247, 2020, doi: 10.1016/j.seppur.2020.116996.

[62] Z. Xue *et al.*, “A novel superhydrophilic and underwater superoleophobic hydrogel-coated mesh for oil/water separation,” *Adv. Mater.*, vol. 23, no. 37, 2011, doi: 10.1002/adma.201102616.

[63] G. Wang, L. Peng, B. Yu, S. Chen, Z. Ge, and H. Uyama, “Hierarchically porous sponge for oily water treatment: Facile fabrication by combination of particulate templates and thermally induced phase separation method,” *J. Ind. Eng. Chem.*, vol. 62, 2018, doi: 10.1016/j.jiec.2017.12.057.

[64] Z. Lei, G. Zhang, Y. Deng, and C. Wang, “Surface modification of melamine sponges for pH-responsive oil absorption and desorption,” *Appl. Surf. Sci.*, vol. 416, 2017, doi: 10.1016/j.apsusc.2017.04.165.

[65] W. Zhang, F. Zhang, S. Gao, Y. Zhu, J. Li, and J. Jin, “Micro/nano hierarchical poly(acrylic acid)-grafted-poly(vinylidene fluoride) layer coated foam membrane for temperature-controlled separation of heavy oil/water,” *Sep. Purif. Technol.*, vol. 156, 2015, doi: 10.1016/j.seppur.2015.09.076.

[66] L. Yu, G. Hao, L. Xiao, Q. Yin, M. Xia, and W. Jiang, “Robust magnetic polystyrene foam for high efficiency and removal oil from water surface,” *Sep. Purif. Technol.*, vol. 173, 2017, doi: 10.1016/j.seppur.2016.09.022.

[67] Z. Maolin, L. Jun, Y. Min, and H. Hongfei, “The swelling behavior of radiation prepared semi-interpenetrating polymer networks composed of polyNIPAAm and hydrophilic polymers,” *Radiat. Phys. Chem.*, vol. 58, no. 4, 2000, doi: 10.1016/S0969-806X(99)00491-0.

[68] J. Wang and S. Liu, “Remodeling of raw cotton fiber into flexible, squeezing-resistant macroporous cellulose aerogel with high oil retention capability for oil/water separation,” *Sep. Purif. Technol.*, vol. 221, 2019, doi: 10.1016/j.seppur.2019.03.097.

[69] Y. Yu, X. Wu, and J. Fang, “Superhydrophobic and superoleophilic ‘sponge-like’ aerogels for oil/water separation,” *J. Mater. Sci.*, vol. 50, no. 15, 2015, doi: 10.1007/s10853-015-9034-9.

[70] H. Y. Mi, X. Jing, A. L. Politowicz, E. Chen, H. X. Huang, and L. S. Turng, “Highly compressible ultra-light anisotropic cellulose/graphene aerogel fabricated by bidirectional

freeze drying for selective oil absorption," *Carbon N. Y.*, vol. 132, 2018, doi: 10.1016/j.carbon.2018.02.033.

[71] C. Wu, X. Huang, X. Wu, R. Qian, and P. Jiang, "Mechanically flexible and multifunctional polymer-based graphene foams for elastic conductors and oil-water separators," *Adv. Mater.*, vol. 25, no. 39, 2013, doi: 10.1002/adma.201302406.

[72] X. Wang *et al.*, "Facile Fabrication of Superhydrophobic and Eco-Friendly Poly(lactic acid) Foam for Oil-Water Separation via Skin Peeling," *ACS Appl. Mater. Interfaces*, vol. 11, no. 15, 2019, doi: 10.1021/acsami.9b02285.

[73] Q. Zhu *et al.*, "Robust superhydrophobic polyurethane sponge as a highly reusable oil-absorption material," *J. Mater. Chem. A*, vol. 1, no. 17, 2013, doi: 10.1039/c3ta00125c.

[74] S. Xiong, Z. Zhong, and Y. Wang, "Direct silanization of polyurethane foams for efficient selective absorption of oil from water," *AIChE J.*, vol. 63, no. 6, 2017, doi: 10.1002/aic.15629.

[75] S. Chatterjee, W. T. Ke, and Y. C. Liao, "Elastic nanocellulose/graphene aerogel with excellent shape retention and oil absorption selectivity," *J. Taiwan Inst. Chem. Eng.*, vol. 111, 2020, doi: 10.1016/j.jtice.2020.04.020.

[76] M. B. Wu *et al.*, "Carboxylated wood-based sponges with underoil superhydrophilicity for deep dehydration of crude oil," *J. Mater. Chem. A*, vol. 8, no. 22, 2020, doi: 10.1039/d0ta03844j.

[77] L. ai Huang, Z. He, J. Guo, S. en Pei, H. Shao, and J. Wang, "Self-Assembled Three-Dimensional Graphene Aerogel with an Interconnected Porous Structure for Lithium-Ion

Batteries," *ChemElectroChem*, vol. 6, no. 10, 2019, doi: 10.1002/celc.201900445.

[78] vahid salimian Rizi, "Ce Pte Us Pt," *Mater. Res. Express*, 2019.

[79] D. E. Ingber *et al.*, "Contributions des recherches en mécanobiologie à la compréhension des mécanismes de la L . T . R . en ostéopathie," *J. Biomech.*, vol. 25, no. 5, 2013.

[80] A. Mata, A. J. Fleischman, and S. Roy, "Characterization of Polydimethylsiloxane (PDMS) Properties for Biomedical Micro/Nanosystems," *Biomed. Microdevices*, vol. 7, no. 4, 2005, doi: 10.1007/s10544-005-6070-2.

[81] Y. Xia and G. M. Whitesides, "Soft lithography," *Annu. Rev. Mater. Sci.*, vol. 28, no. 1, 1998, doi: 10.1146/annurev.matsci.28.1.153.

[82] J. N. Lee, C. Park, and G. M. Whitesides, "Solvent Compatibility of Poly(dimethylsiloxane)-Based Microfluidic Devices," *Anal. Chem.*, vol. 75, no. 23, 2003, doi: 10.1021/ac0346712.

[83] S. Jung *et al.*, "Reverse-micelle-induced porous pressure-sensitive rubber for wearable human-machine interfaces," *Adv. Mater.*, vol. 26, no. 28, 2014, doi: 10.1002/adma.201401364.

[84] W. Liu *et al.*, "3D Porous Sponge-Inspired Electrode for Stretchable Lithium-Ion Batteries," *Adv. Mater.*, vol. 28, no. 18, 2016, doi: 10.1002/adma.201505299.

[85] S. J. Choi *et al.*, "A polydimethylsiloxane (PDMS) sponge for the selective absorption of oil from water," *ACS Appl. Mater. Interfaces*, vol. 3, no. 12, 2011, doi: 10.1021/am201352w.

[86] C. C. Ong, S. Sundera Murthe, N. M. Mohamed, V. Perumal, and M. S. Mohamed Saheed,

"Nanoscaled Surface Modification of Poly(dimethylsiloxane) Using Carbon Nanotubes for Enhanced Oil and Organic Solvent Absorption," *ACS Omega*, vol. 3, no. 11, 2018, doi: 10.1021/acsomega.8b01566.

[87] J. González-Rivera, R. Iglio, G. Barillaro, C. Duce, and M. R. Tinè, "Structural and thermoanalytical characterization of 3D porous PDMS foam materials: The effect of impurities derived from a sugar templating process," *Polymers (Basel).*, vol. 8, no. 6, pp. 1–13, 2018, doi: 10.3390/polym10060616.

[88] P. F. Ibáñez-Ibáñez, F. J. Montes Ruiz-Cabello, M. A. Cabrerizo-Vílchez, and M. A. Rodríguez-Valverde, "Contact line relaxation of sessile drops on PDMS surfaces: A methodological perspective," *J. Colloid Interface Sci.*, vol. 589, 2021, doi: 10.1016/j.jcis.2020.12.093.

[89] J. P. Deville and C. S. Cojocaru, "Spectroscopic Analyses of Surfaces and Thin Films," in *Materials Surface Processing by Directed Energy Techniques*, 2006. doi: 10.1016/B978-008044496-3/50013-7.

[90] B. Gayani, D. Senarathna, M. M. Weerasekera, N. Kottegoda, and D. R. Ratnaweera, "Improving superhydrophobicity of polydimethylsiloxanes using embedding fluorinated polyhedral oligomeric silsesquioxanes cages," *SN Appl. Sci.*, vol. 2, no. 12, 2020, doi: 10.1007/s42452-020-03721-y.

[91] D. C. Nguyen, T. T. Bui, Y. B. Cho, and Y. S. Kim, "Highly hydrophobic polydimethylsiloxane-coated expanded vermiculite sorbents for selective oil removal from water," *Nanomaterials*, vol. 11, no. 2, 2021, doi: 10.3390/nano11020367.

[92] L. M. Al-Harbi, M. S. A. Darwish, M. M. Khowdiary, and I. Stibor, "Controlled preparation

of thermally stable Fe-poly(dimethylsiloxane) composite by magnetic induction heating," *Polymers (Basel).*, vol. 10, no. 5, 2018, doi: 10.3390/polym10050507.

[93] A. N. Parvez, M. H. Rahaman, H. C. Kim, and K. K. Ahn, "Optimization of triboelectric energy harvesting from falling water droplet onto wrinkled polydimethylsiloxane-reduced graphene oxide nanocomposite surface," *Compos. Part B Eng.*, vol. 174, 2019, doi: 10.1016/j.compositesb.2019.106923.

[94] J. Nourmohammadi, T. Hajibabaei, G. Amoabediny, S. H. Jafari, and N. Salehi-Nik, "Aminosilane layer formation inside the PDMS tubes improves wettability and cytocompatibility of human endothelial cells," *Trends Biomater. Artif. Organs*, vol. 29, no. 2, pp. 123–131, 2015.

[95] K. Malecha, I. Gancarz, and L. J. Golonka, "A PDMS/LTCC bonding technique for microfluidic application," *J. Micromechanics Microengineering*, vol. 19, no. 10, 2009, doi: 10.1088/0960-1317/19/10/105016.

[96] R. Goseki, L. Hong, M. Inutsuka, H. Yokoyama, K. Ito, and T. Ishizone, "Synthesis and surface characterization of well-defined amphiphilic block copolymers composed of polydimethylsiloxane and poly[oligo(ethylene glycol) methacrylate]," *RSC Adv.*, vol. 7, no. 41, pp. 25199–25207, 2017, doi: 10.1039/c7ra02569f.

[97] X. Le, W. Lu, J. Zhang, and T. Chen, "Recent Progress in Biomimetic Anisotropic Hydrogel Actuators," *Advanced Science*, vol. 6, no. 5. 2019. doi: 10.1002/advs.201801584.

[98] K. Sano, Y. Ishida, and T. Aida, "Synthesis of Anisotropic Hydrogels and Their Applications," *Angewandte Chemie - International Edition*, vol. 57, no. 10. 2018. doi: 10.1002/anie.201708196.

[99] T. Tanaka, I. Nishio, S. T. Sun, and S. Ueno-Nishio, “Collapse of gels in an electric field,” *Science (80-.).*, vol. 218, no. 4571, 1982, doi: 10.1126/science.218.4571.467.